Encapsulation of Pancreatic Islets/Nanoparticles within Biofunctional Poly (ethylene glycol) (PEG) Hydrogel

by

Caner Nazlı

A Thesis Submitted to the
Graduate School of Engineering
in Partial Fulfillment of the Requirements for
the Degree of

Master of Science
in
Material Science and Engineering

Koc University

September 2011

Koc University

Graduate School of Sciences and Engineering

This is to certify that I have examined this copy of a master's thesis by

Caner Nazlı

and have found that it is complete and satisfactory in all respects,
and that any and all revisions required by the final
examining committee have been made.

Committee Members:

_____

Seda Kızılel, Ph. D. (Advisor)

_____

H. Funda Yağcı Acar, Ph. D.

_____

Başak Kayıtmazer, Ph. D.

Date: _____

07.09.2011

ABSTRACT

Poly (ethylene glycol) **(**PEG) hydrogels have been extensively used in biomedical engineering, pharmaceutical applications, and biomaterial science due to their tunable structure, desirable mechanical features, high water content, and biocompatibility. In this study, the process of cell or nanoparticle coating through surface initiated photopolymerization is described. First, PEG hydrogel was synthesized on photoinitiator immobilized silicon surfaces, and physical properties such as swelling and thickness have been characterized. Next, surface initiated photopolymerization technique has been applied for the coating of pancreatic islets and magnetic iron oxide nanoparticles (MIONPs) within biomolecule functionalized PEG hydrogel, respectively. Viability and functionality assays demonstrated that islets coated within insulinotropic ligand functionalized PEG hydrogel have enhanced insulin secreting capability compared to control islets. Cell adhesion ligand functionalized PEG hydrogel coated MIONPs have also been investigated to assess their effect on HeLa cell viability and cellular uptake. These results suggest that the presence of cell adhesion domains within PEG hydrogel structure shows no toxicity to HeLa cells as well as improves cellular uptake of MIONPs by HeLa cells. In conclusion, coating of islets within functional PEG hydrogel before implantation may enhance functionality of transplanted islets and reduce the clinical transplantation volume, and coating of nanoparticles within functional PEG hydrogel may improve tumor detection as a result of enhanced MIONPs uptake by tumor cells.

ÖZET

PEG hidrojelleri, ayarlanabilir yapıları, mekanik özellikleri, yüksek su tutma kapasiteleri ve biyo uyumlulu olmaları sayesinde biyomedical mühendisliği, ilaç uygulamaları, biyomateryal bilimi alanlarında yaygın olarak kullanılmaktadırlar. Bu çalışmada, yüzeyden başlayan polimerizasyon yöntemi kullanılarak hücre ve nanoparçacık yüzeylerini PEG hidrojeli ile kaplama yöntemi geliştirilmiştir. İlk etapta, PEG hidrojeli, şişme ve kalınlık özellikleri bakımından incelenmek amacıyla, photo başlatıcı tespit edilmiş silicon yüzey üzerinde oluşturulmuştur. Sonrasında, bu teknik pankreas adacıklarını ve manyetik demir oksit nanoparçacıklarını biyolojik işlev gösterebilen PEG hidrojeli ile kaplamak üzere düzenlenmiştir. Uygulanan canlılık ve biyolojiik işlev testleri yardımıyla, insulin sentezlenmesini destekleyen biyolojik molekül bağlı PEG hidrojeli kaplanmış adacıkların, kontrol grubu adacıklarına göre insulin sentezleme yeteneklerinin önemli şekilde arttığı gözlenmiştir. Hücre yapışma biyolojik molekülü bağlı PEG hidrojeli kaplanmış nanoparçacıkların ise toksik etki göstermemelerinin yanında hidrojel ile kaplanmamış nanoparçacıklara göre yüksek oranda HeLa hücrelerine girebildikleri belirlenmiştir. Sonuç olarak, biyolojik işlevli PEG hidrojeli kaplama teknolojisinin hem adacık kaplanmasında hem de nanoparçacık kaplanmasında, verimli şekilde uygulanabileceği gösterilmiştir.

ACKNOWLEDGEMENTS

I would like to thank Assist. Prof. Dr.Seda Kızılel for her supervision, advices and superior guidance. During the last two years, I had a great opportunity to learn many things our research field from her.

I would like to thank gratefully my committee member Assoc. Prof. Dr. H. Funda Yağcı Acar for her generous encourage allowing me to use the chemicals and devices in her laboratory during the study. I also want to send my special thanks to other committee member Assist. Prof. Dr. Başak Kayıtmazer for her advice about my thesis and for serving in my thesis committee.

I would like to thank to Prof. Dr. A. Levent Demirel for his support and comments about this study. Special thanks to his master student and my hearty friend H. Enis Karahan for his heps in DLS, Zeta potential measurement, AFM studies and advices about manuscript, and to his undergraduate student Lütfiye Eyüboğlu for her generous helps.

I would like to thank to Assoc. Prof. Dr. Ali Osman Gürol from Istanbul University Medical School for islet isolation. I also benefited by outstanding works from T. İpek Ergenç, N. Ezgi Sarıkaya and Dilruba İnam with their particular skills in handling experiments. Furthermore, I would like to express my sincere gratitude to Dr. Rıza Kızılel and my energetic friend Selimcan Azizoğlu for giving motivation and enthusiasm to me about this study.

In addition, it is a pleasure to pay tribute also to my colleagues who supported me in any part of the project. To Recep Kaş, Cansu Yıldırım and İbrahim Hocaoğlu I would like to thank for the scientific discussions. To Yasemin Yar thanks for the preparation of nanoparticles. To Selçuk Acar thanks for ICP measurement. To Hande Öztürk, thanks for her technical support and advices about the experiment.

TABLE OF CONTENTS

LIST OF TABLES

LIST OF FIGURES

ABBREVIATIONS

MW	Molecular Weight
EY	Eosin Y
WRK	Woodward's Reagent K
RT	Room Temperature
PEG	Poly (ethylene glycol)
PEGDA	Poly (ethylene glycol) diacrylate
TEA	Triethanolamine
VP	1-Vinyl 2-pyrrolidone
HG	Hydrogel
UV	Ultraviole
FDA	Food and Drug Administration
APTES	Aminopropyl-Triethoxysilane
APTMS	3-(aminopropyl) trimethoxysilane–tetramethoxysilane
TIDM	Type I Diabetes Mellitus
IgA	Immunoglobulin A
IgB	Immunoglobulin B
GLP-1	Glucagon-like-peptide-1
BSA	Bovine Serum Albumin
ELISA	Enzyme-Linked Immunosorbent Assay
NPs	Nanoparticles
ENPs	Encapsulated Nanoparticles
MIONPs	Magnetic Iron Oxide Nanoparticles
EMIONPs	Encapsulated Magnetic Iron Oxide Nanoparticles
MRI	Magnetic Resonance Imaging
NMWL	Nominal Molecular Weight Limit
PPS	Prepolymer Solution
UV-Vis	Ultraviole - Visible
FT-IR	Fourier transform infrared
DLS	Dynamic Light Scattering
AFM	Atomic Force Microscopy
ICP-OES	Inductively Coupled Plasma Optical Emission Spectrometry
P	PEG-Peptide Conjugate
PPS	Prepolymer Solution
Ref	Reference

Chapter 1

INTRODUCTION

Hydrogels have been extensively used in biomedical engineering, pharmaceutical applications, and biomaterial science due to their tunable structure, desirable mechanical features, high water content, and biocompatibility [1-2]. The most widely exploited synthetic hydrogels are composed of poly (ethylene glycol) (PEG). PEG, which is an FDA approved material with well-known biocompatibility and low-toxicity properties, is an attractive substance with unique properties and have extensive use in biomaterials, biotechnology, and medicine fields [3]. PEG hydrogel does not only show resistance to cell and protein adhesion, but minimizes recognition by immune cells, which makes PEG hydrogel appropriate for applications such as scaffold for tissue engineering, coating material for cell encapsulation and nanoparticle encapsulation [4-6].

The remarkable features of PEG hydrogel make it significant material for biomedical applications, such as tissue and cell engineering, drug delivery and hyperthermia. PEG hydrogels are used in tissue engineering field as scaffolds for repairing and regeneration of tissues and organs [4, 7]. PEG hydrogel could also be used for encapsulation of pancreatic islets to prevent immune rejection after transplantation [1, 5]. Recently, it was employed for development of the biocompatible magnetic hydrogel composites for hyperthermia in cancer therapy [6].

Encapsulation of pancreatic islets has been considered for the treatment of type I diabetes mellitus. Semi-permeable PEG hydrogel membranes can function as an immune-camouflage barrier depending on the principle that the semi-permeable hydrogel allows for the diffusion of oxygen and nutrients while hindering immune cells and proteins [8]. However, the lack of long term viability and functionality of transplanted islets, and high transplanted graft volume prevent clinical application of islet transplantation [9]. Covalent incorporation of biomolecules into PEG based synthetic hydrogels is a powerful method to overcome difficulties associated in cellular therapy [10].

Another biomedical application of PEG hydrogels that is relevant to this work includes nanoparticles for the detection of tumors. Successful exploitation of nanoparticles (NPs) have been frequently hindered in clinical applications due to agglomeration in physiological condition or fast detection via immune cells [11]. PEG hydrogel encapsulation can be suitable for coating NPs as well as magnetic iron oxide nanoparticles (MIONPs) in order to use them in biological environment. MIONPs have been extensively used as magnetic resonance imaging (MRI) contrast agent and targeted drug delivery tool. However, MIONPs tend to agglomerate and adsorb plasma proteins while circulating in blood. Hence, MIONPs are not allowed to reach target tissue by some biological systems such as reticuloendothelial system, vascular endothelium or blood brain barrier [12]. Targeting ligands could be incorporated to the nanoparticle surface to enhance the efficiency of cellular delivery and specific intracellular targeting [13]. Therefore, cell adhesion binding domain functionalized PEG hydrogel coating around MIONP can enhance attachment of encapsulated NPs to cell membrane and intracellular uptake in target tissues.

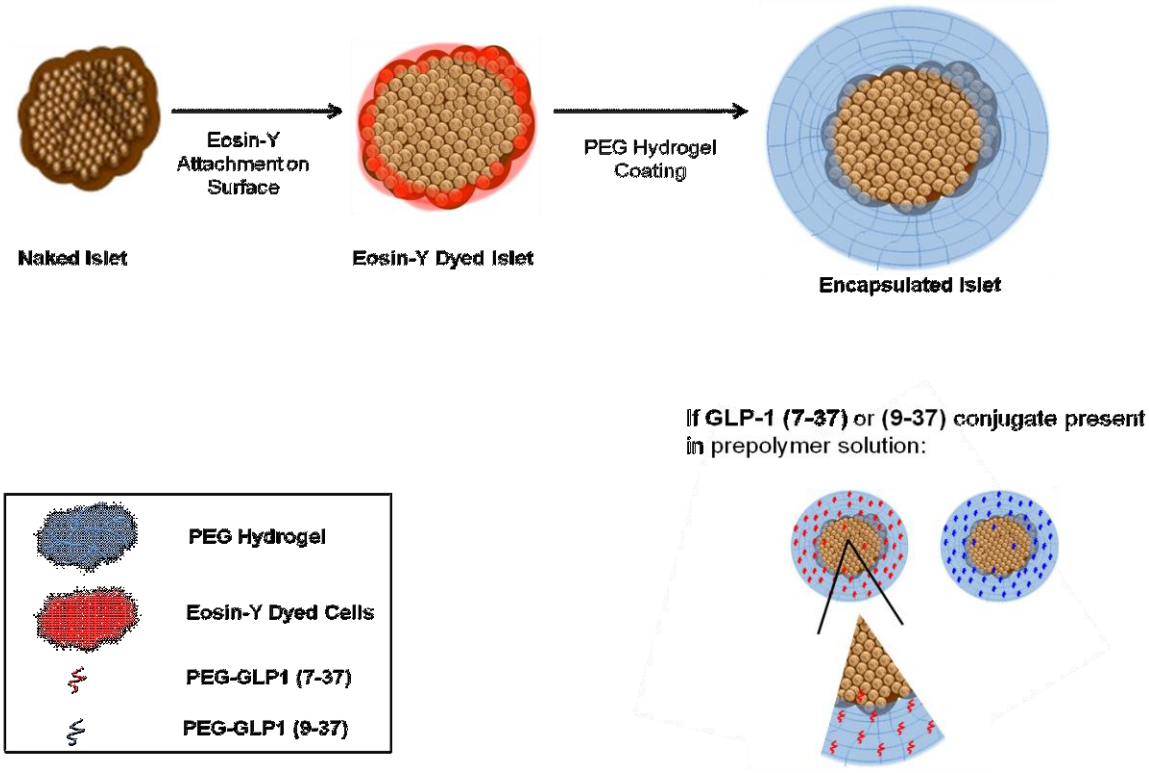

Figure 1.1 – Schematic illustration of encapsulation of pancreatic islets within biofunctional PEG hydrogel

In the beginning of this thesis, biofunctional PEG hydrogel was synthesized on photoinitiator functionalized surfaces in order to investigate its physical properties such as swelling and thickness. Next, pancreatic islets have been coated within biofunctional PEG hydrogel via surface initiated photopolymerization in order to address difficulties involved in host rejection, islet viability and long-term functionality. Figure 1.1 demonstrates the process of the production glucagon-like-peptide (GLP-1) conjugates functionalized PEG hydrogel encapsulated Islets. GLP-1 has been considered as a biomolecule in this study due to its well established glucose dependent insulinotropic effect on pancreatic beta-cells and positive effects on preventing islet apoptosis [14]. This promising method allows for coating of islets within biofunctional semi-permeable hydrogel membrane to prevent diffusion of components of the immune system and to exchange nutrients and wastes with long-term insulin secretion function.

In the second part of this thesis, MIONPs have been encapsulated within biofunctional PEG hydrogel via surface initiated photopolymerization method in order to address difficulties involved in MIONPs biodistribution and cellular uptake. Figure 1.2 illustrates the process of the manufacturing biofunctional PEG hydrogel encapsulated MIONPs. This novel method does not only allow coating of MIONPs within nano-thin hydrogel layers which may prevent undesirable cell and protein adhesion due to the presence of PEG hydrogel, but also may allow for cellular uptake in target tissue in a specific manner as a result of presence of covalently bonded cellular adhesion peptides (RGDS) within the hydrogel network. Biofunctional PEG hydrogel coating which can prevent agglomeration of NPs and increase blood circulation time will be significant tool for diagnostic and therapeutic imaging technologies as well as targeted drug delivery area.

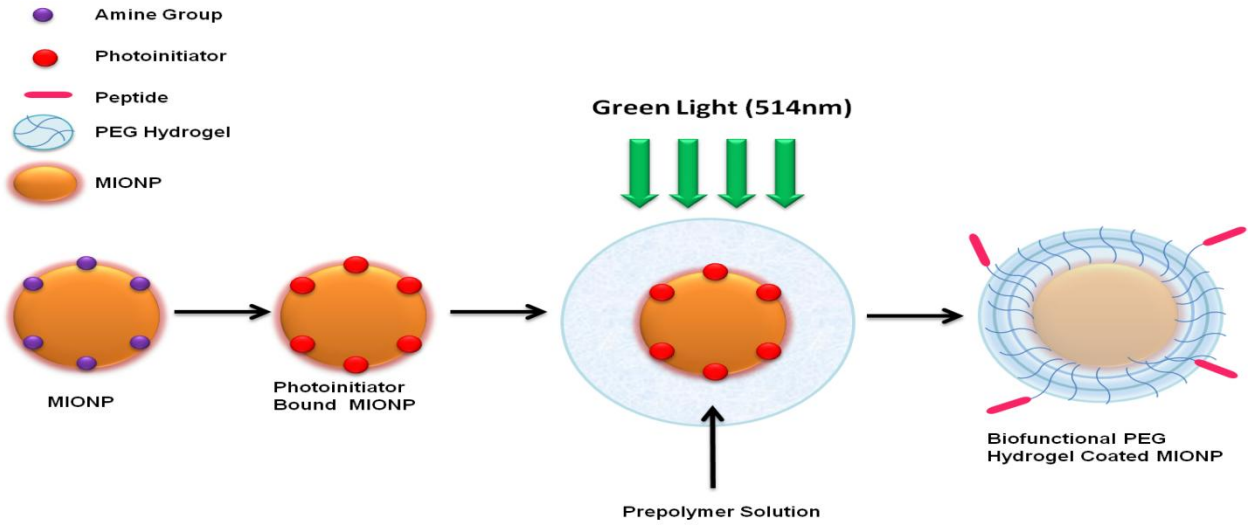

Figure 1.2 - Schematic diagram of encapsulating MIONP within biofunctional PEG hydrogel

Chapter 2

Literature Review

2.1. Properties and Applications of PEG Hydrogels

2.1.1. Hydrogels

Hydrogel structure is a water-swollen network which consists of water (hydro) and water-insoluble hydrophilic polymer network (gel) [1, 15-16]. Hydrogels can swell in water as opposed to dissolving in water, because they consist of cross-linked polymer network structure [17]. Because of their resemblance to natural extracellular matrix (ECM), hydrogels have been explored widely for medical applications since Wichterle and Lim initially produced hydrogel that was composed of cross-linked poly(2-hydroxyethyl methacrylate) in 1960s [15]. Then, a variety of synthetic and naturally inspired materials are used to produce hydrogel [18]. Poly(ethylene glycol) (PEG), poly(vinyl alcohol) (PVA), poly(acrylic acid) (PAA), poly(propylene furmarate-co-ethylene glycol) (P(PF-co-EG)), and polypeptides are exploited to synthesize of synthetic hydrogels. Agarose, alginate, chitosan, collagen, fibrin, gelatin and hyaluronic acid are also expoited to manufacture natural hydrogels [15, 18]. *In vivo* applications of natural hydrogels are constrained ascribed to their potential causing immune rejection and infection [18]. As opposed to natural ones, synthetic materials are favorable for making hydrogels because their chemistry and physical features are manageable and reproducible [15]. By means of these properties, gel production dynamics, cross-linking density, mechanical and degradation characters of synthetic hydrogels can be adjusted [15]. Synthetic hydrogels exhibit physical properties similar to tissues due to their high water content, soft and robbery uniformity, and low surface tension with water or biological fluids [17].

Hydrogels acquire expanding notice due to their capability to absorb a large amounts of water, biocompatibility, low surface tension, inconsiderable mechanical and frictional irritation [15]. The affinity of hydrogels to water is ascribed to the existence of hydrophilic groups such as -OH, -$CONH_2$-, and -SO_3H constructing hydrogel structures [17]. When hydrogels are exposed to

liquid environment, cross-linked network hinders the dissolution of the hydrogels and adsorbed water causes swelling [19].

Mechanical durability of the hydrogels is significant in body fluid. The hydrogel must be capable of preserving their physical integrity and mechanical strength in physiological environment in order to become a useful biomaterial [20]. The strength of the hydrogels can be adjusted via adding co-monomers and increasing degree of cross-linking [20]. On the other hand, hydrogels could be degradable and ultimately can break down in response to an external stimuli such as a change in pH, temperature or a bulk molecule concentration [7]. Hydrogels can degrade with different mechanisms such as hydrolysis, enzymatic cleavage and dissolution. Synthetic hydrogels are subject to degradation via hydrolysis of ester linkages resulting in the analogous hydroxyl acids as non-toxic degradation products [1]. In order to fabricate degradable hydrogel network, linkers which consist of degradable sequence could be incorporated into the precursor (prepolymer) solution [19].

Hydrogels that will be used for medical implantation must be non-toxic and non-immunogenic [15]. Due to their hydrophilic nature, most synthetic hydrogels hinder adsorption of ECM proteins. Hydrogels can provide an suitable environment to direct cell movement, proliferation, and differentiation [15]. Hydrogel precursor solution is in liquid form before gelation. This allows incorporation of therapeutic agents such as cells, proteins and drugs into polymer solution, providing high loading and homogenous distribution within the cross-linked network [15].

Figure 2.1 - Schematic illustration of method for formation of hydrogels

Hydrogels demonstrate similarities with natural extracellular matrix in terms of mechanical and structural features, and can be produced under relatively mild conditions [15]. General route of the hydrogel synthesis is shown in figure 2.1 in which water soluble polymer chains are cross-

linked to produce hydrogel network. Polymer cross-linking reaction can be induced by radiation or chemical reaction [15]. The radiation reactions are initiated via electron beams, gama-rays, X-rays, UV or visible light. The chemical reactions are initiated via small molecular weight cross-linking agents that bind monomers. Synthetic materials used for producing hydrogels allow for photopolymerization, adjusting mechanical properties and control of chemical composition [18].

These desirable features of hydrogels are the reason behind their wide range of applications from food additives to clinical applications. As a result of demonstrating biocompatibility, hydrogels are used for contact lenses, burn wound dressing and coating for cells [20]. Thus, hydrogels are appropriate for coating of bio-structures such as proteins, cells etc… without changing physical and chemical properties of the biomolecules or cells [15].

2.1.2. PEG Hydrogels

Poly (ethylene glycol) (PEG) hydrogel is the most widely exploited synthetic material. (figure 2.2). PEG which is an FDA approved material with well-known biocompatibility and low-toxicity properties is an attractive substance with unique properties and has extensive use in biomaterials, biotechnology, and medicine [3]. By means of its high hydrophilicity, PEG demonstrates resistance to cell and protein adhesion *in vivo* [15, 18]. PEG has exceptional features such as linearity of structure, non-ionic nature and water solubility. These properties provide a high level of polymer-solvent interaction in water [21]. Water solubility of PEG depends on perfect structural suitability between water and polymer [21]. Ethylene segments permeate spaces in the water structure and disturb nominally the structure of water [21]. There are many potential features regarding protein resistance of PEG in aqueous environment. PEG has minimum surface energy in water. Minimum interfacial energy diminishes the driving force of the protein adhesion. Also, proteins have low interfacial energy. As a result of these, non-specific interactions between PEG and proteins do not occur frequently. PEG segments are not hampered sterically in water and are highly mobile [21]. Hence, coating of surfaces interacting with blood stream using PEG has been demonstrated as a useful strategy to minimize protein adhesion on surfaces. PEG is also commercially available with wide range of molecular weight from 200 to several million [21].

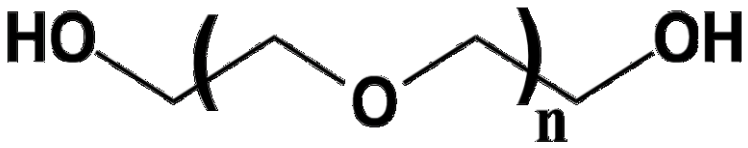

Figure 2.2 – PEG structure

PEG hydrogels can be generated by cross-linking of water soluble PEG chains via free-radical polymerization. Free-radical polymerization progresses via a chain mechanism, which includes four distinct types of reactions including free radicals [22]:

1) Radical formation from non-radical chemicals (initiation)

2) Radical binding to a substituted alkene group (propogation)

3) Atom transfer and atom abstraction reactions (chain transfer and termination by disproportionation)

4) Radical-radical recombination reactions (termination by combination).

Extensive literature work has been devoted to improve photoinitiated free radical polymerization. Photoinitiated polymerizations are practical approaches for biomaterial synthesis because these types of reactions require mild conditions (at RT and neutral pH) [23]. PEG could be covalently cross-linked via photoinitiator mechanism such as acetophenone/UV light or eosin Y (EY) and triethanolamine/visible blue light system [23]. PEG hydrogels synthesized via photopolymerization consist of ester bonds for hydrolysis [18]. Polymer fraction, polymer size, cross-linker concentration, and light exposure time which have effect on hydrogel porous structure property [15] are adjustable in photoinitiated free radical polymerization method.

Toxicity of chemical cross-linking reaction is an important concern because the precursor solution contains reactive groups and compounds such as initiators, co-cross-linkers and organic solvents. Photopolymerization with visible light suggests spatial and temporal control of the cross-linking reaction without toxicity to living cells. During photoinitiated polymerization (figure 2.3), light exposure generates reactive species that initiate cross-linking reaction. These radicals induce radical chain polymerization. Next, radical fragments propagate with monomers in the system to make longer radicals of any size.

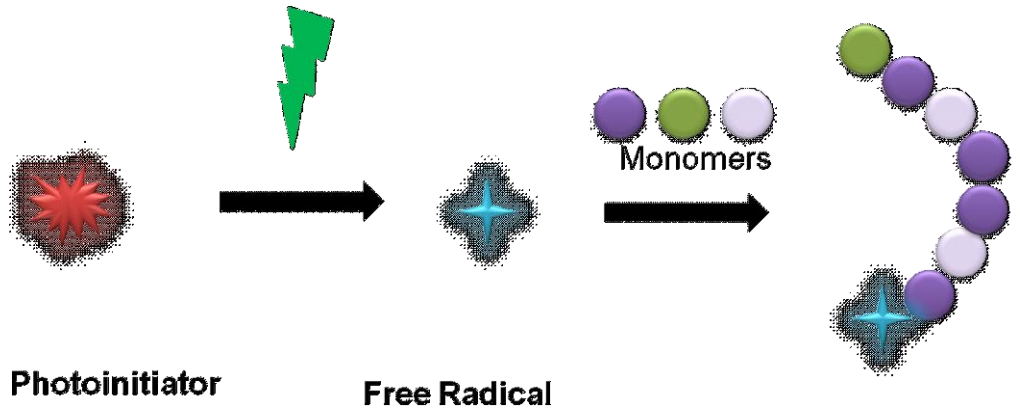

Figure 2.3 - General representation of radical formation during photoinitiation

Radicals may also terminate with another radical either via combination or disproportionation in order to form a cross-link. PEG hydrogel formation via photopolymerization is a nonlinear polymerization reaction where excessive branching and cross-linking reaction lead to gel formation. The cross-linking reaction take places due to the presence of bifunctional PEG monomer, with two acrylate double bonds at both ends of PEG polymer (figure 2.4).

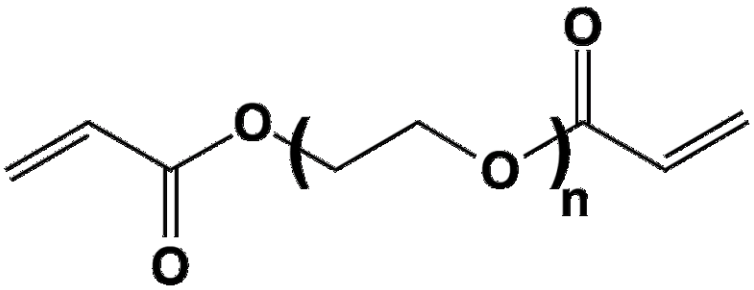

Figure 2.4 – PEGDA structure

Hydrogels can be manufactured in variety of geometries such as slabs, cylinders, films, microspheres and nanospheres [19]. These features of hydrogels make them significant materials for biomedical applications, such as tissue engineering, drug delivery and *in vivo* imaging. Hydrogels are used in tissue engineering area as a scaffold for repairing and regenerating of tissues and organs [7]. For example, PEG hydrogel was used as a scaffold for differentiation of osteoblast to bone [5]. Hydrogels are promising tools for drug delivery application because they allow for the controlled release of therapeutic agents [24]. Hence, physicochemical and biological features of hydrogels, together with their great variety provide these polymeric materials as exceptional candidates for therapeutic agent delivery systems [17].

Natural and synthetic hydrogels have gained great interest for encapsulation of cells [7]. In 1980, Lim and Sun fabricated calcium alginate hydrogel microcapsules for cell encapsulation, specifically pancreatic islets [7]. PEG hydrogel could be used for encapsulation of pancreatic islets to prevent immune rejection after transplantation [1]. PEG hydrogel chemistry and kinetic mechanism also allows for versatile hydrogel formation and incorporation of biomolecules in order to produce biofunctional PEG hydrogel systems. In next section, biomedical applications of PEG hydrogels such as encapsulation of pancreatic Islets and coating MIONPs will be discussed in detail.

2.1.3. Biomedical Applications of PEG Hydrogels

2.1.3.1. Encapsulation of Pancreatic Islets within Biofunctional PEG Hydrogel for Treatment T1DM

Diabetes continues to be destructive diseases, with its huge cost in terms of human enduring and health care expenses [25]. Type-1 diabetes mellitus (T1DM), which occurs as a result of destruction of pancreatic islets by the immune system either due to stress or by chemical means, leads to insulin deficiency [26]. Adams et al. (2010) asserted that failure of the immunity system emanated from infection of bacteria or viruses results in autoimmune diseases. Environmental and genetic factors play a vital role in breakdown the immune system. Richer and Horwits demonstrate that Coxsackieviruses could bring about type 1 diabetes because of the homology between Coxsackievirus protein PC-2 and the islet antigen GAD65 [27]. Although, insulin cure has notably eliminated the direct risk of T1DM, the chronic effects of diabetes prolong to be ambiguous. Since, insulin therapy leads to chronic complications such as cardiovascular diseases, rental failure, amputation and blindness, alternative approaches should be developed to provide glycemic control for patients with T1DM [28].

Transplantation of pancreatic islets is an attractive promising technique for the treatment of T1DM [29] since Pybus (1882-1975) endeavored to implant pancreatic tissue to ameliorate diabetic patients [30]. However, several obstacles confronted during islet transplantation decrease islet viability and function for long time [31]. As soon as the tissue is implanted, immune attack to grafted islets occurs [32]. Since, T cell clones regularly scrutinize the existence of viral peptide. When these recognize viral peptides on the implanted cell surface, they attack to kill the

implanted tissue. During this self check, T cells identify histocompatibility antigens on the implanted tissue as virus infection and as a result, cytotoxic T cells reject implanted cells [27].

One of the applications of PEG in biomedical area is microencapsulation of pancreatic islets within PEG hydrogels to protect islets from immune attack for the treatment of T1DM [33]. The aspire to islet transplantation without requirement of immunosuppression, has resulted in the improvement of semi-permeable PEG hydrogel systems which provide protecting transplanted islets from the host immune system (immune cells and IgA-IgB) whereas permitting diffusion of glucose, insulin, oxygen, essential nutrients and metabolic products (figure 2.5) [9]. Microencapsulation suggests an optimal volume-to-surface ratio for rapid exchange of hormones and nutrients. Diffusion behaviors of proteins through PEG hydrogels demonstrated that gels produced with the suitable formulation could be used immunocamouflage [25]. However; several hindrances such as high transplantation volume, lack of long-term viability and functionality were confronted in clinical application of encapsulated islets. Covalent attachment of peptide sequences within synthetic hydrogels provides addition of attractive physical or biological properties in the system [34]. So, covalent conjugation of insulinotropic peptides into PEG hydrogel is promising method to solve obstacles such as maintaining islet viability, functionality and high transplantation volume.

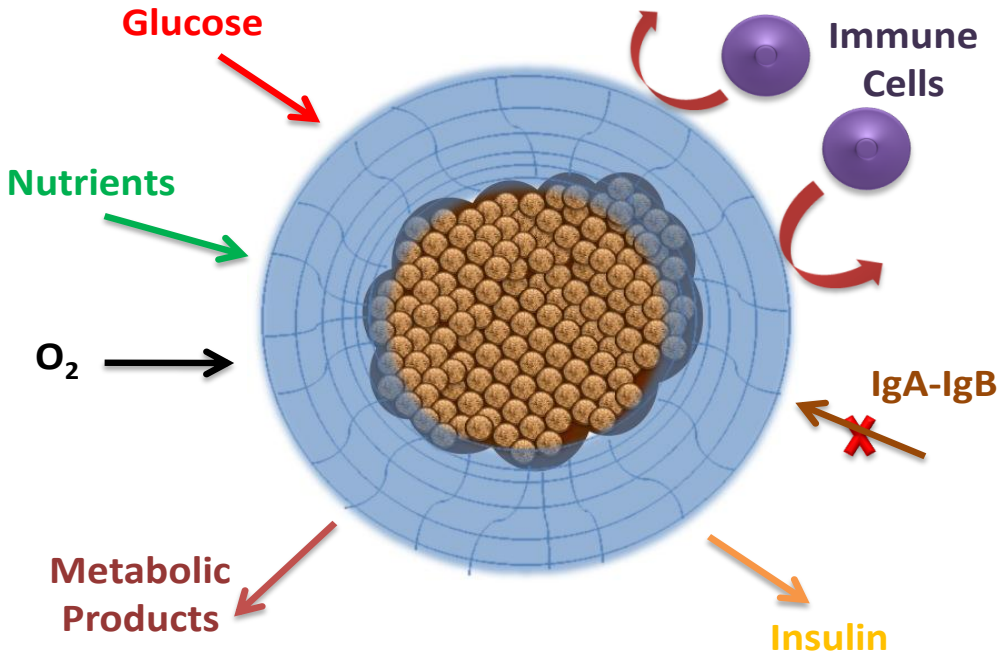

Figure 2.5 - Schematic of immunoprotection via a permselective PEG hydrogel membrane

2.1.3.2. Encapsulation of MIONPs within Biofunctional PEG Hydrogel for Biomedical Applications

Nanoparticles are powerful candidates to alter current clinical diagnostic and therapeutic methods. Magnetic iron oxide nanoparticles (MIONPs) have broad variety of applications in the areas such as cancer, cardiovascular disorders and neurological disorders [12]. Specifically, MIONPs have been exploited widely in biotechnology and medicine as delivery systems for drugs, genes, biomolecules, stem cell tracking, and diabetes treatment, hyperthermia and the detection of cancer [11, 35]. In addition to *in vivo* application, MIONPs are useful for various *in vitro* applications in medical diagnostics such as magnetic separation of cells, proteins, DNA/RNA, and other biomolecules [11]. Although MIONPs find extensive application areas in biomedicine and analysis methods, they have been hindered in clinical applications due to agglomeration in physiological condition and fast detection by immune cells [11, 36]. MIONPs without surface coating exhibit hydrophobic surface property with a large surface area to volume ratio [36-38]. So, these particles tend to agglomerate and form larger clusters [11, 39] which are not appropriate for biomedical applications due to short circulation half-life [11] [36] and exhibition of ferromagnetic behavior without magnetic field [37]. Hence, MIONPs are not allowed to reach target tissue by some biological systems such as reticuloendothelial system, vascular endothelium or blood brain barrier [12]. Therefore, coating of the MIONPs within biofunctional synthetic membrane could improve their distribution in aqueous environment [40].

Different types of post-synthesis coating approaches have been improved for stabilization and functionalization of MIONPs such as monolayer ligands, polymers and silica coatings [13]. Biocompatible polymers such as PEG and polyvinylpyrrolidone are extensively exploited as encapsulating materials for MIONPs [11, 39]. Particularly, PEG-coated MIONPs demonstrate appropriate stability in the physiological environment [11]. Researchers have shown that PEG coating of NPs improves their half-life in body and increases the efficiency of their uptake [11, 36, 41]. It has also been observed that the magnetic field strength on the surface of magnetic nanoparticles depends on coating material property. For example, dextran coating decreased the magnetic field strength of iron oxide nanoparticles due to decreased interaction between iron

oxide nanoparticles and water molecules [40]. Consequently, a coating structure with high water content is desirable to utilize MIONPs with maximum efficiency.

The remarkable properties of PEG hydrogels mentioned in previous section make PEG hydrogels indispensable in tissue engineering, biomedical implants, drug delivery, and bionanotechnology [1-2]. PEG hydrogels supply a highly-swollen three-dimensional structure with their elastic network like soft tissues. The most preferred method to make PEG hydrogel is photopolymerization. In this strategy, interaction with light converts PEG macromer solutions into solid hydrogels at physiological pH. This technique allows tuning mechanical properties, chemical compositions, thickness and swollen features of the PEG hydrogels [18]. Therefore, PEG hydrogel encapsulation using photopolymerization can be suitable for coating NPs as well as MIONPs in order to use them in biological environments. PEG hydrogel does not only show resistance of cell and protein adhesion, but also prevent diffusion of components of immune system such as immune cells and immune system proteins with the specific design of a network mesh size [4-6, 42].

In order to induce cellular delivery and specific intracellular targeting, specific ligands could be incorporated onto nanoparticle surface [13, 38]. Target molecules for reaching tumor area should exist at adequate density on the surface of the membrane of vascular endothelium in solid tumors, but lack endothelial cells in healthy tissues such as fibroblast growth factor, vascular endothelial growth factor and various integrins [43]. In this study, we hypothesized that cell binding peptide functionalized PEG hydrogel coating could enhance binding of MIONPs to cell membrane and cellular uptake in target tissues. Biofunctional PEG hydrogel encapsulated MIONPs are nanosized magnetic hydrogel particles with core-shell structure, which includes magnetic cores, cross-linked PEG shell and covalently bound RGDS (Arg-Gly-Asp-Ser) peptide. RGDS is cell binding sequence of fibronectin [44]. It provides binding to $\acute{\alpha}_v\beta_3$ integrin which is located at the outer cell membrane of the tumor endothelial cells [12, 43, 45]. Subsequently, binding RGDS on the MIONPs can be useful to increase efficiency of internalization of them into tumor area [46]. The PEG hydrogel shell prevents agglomeration, cell and protein adhesion, while RGDS peptide provides targeting cancer cells and enhancing cellular uptake.

2.1.4. Synthesis of PEG Hydrogel

In this thesis, we applied an experimental technique which was developed recently by Kizilel et al. (2004) [3] to produce biofunctional PEG hydrogel for coating around pancreatic islets and MIONPs. In this surface initiated polymerization method, first, surface bound EY (photoinitiator) is excited to its triplet state via green light (514nm). Electron transfer and proton loosing occur from the triethanolamine (TEA) (co-initiator) to the excited EY result in formation of the neutral alpha amino radical TEA (TEA*) (figure 2.7-A). Generally it is assumed that TEA* initiates free radical polymerization [3]. In this system, as a result of co-polymerization of PEGDA monomer with 1-vinyl 2-pyrrolidone (VP), covalently cross-linked hydrogel is obtained where excessive branching and cross-linking reactions led to gel formation. [9, 47] (figure 2.7-B).

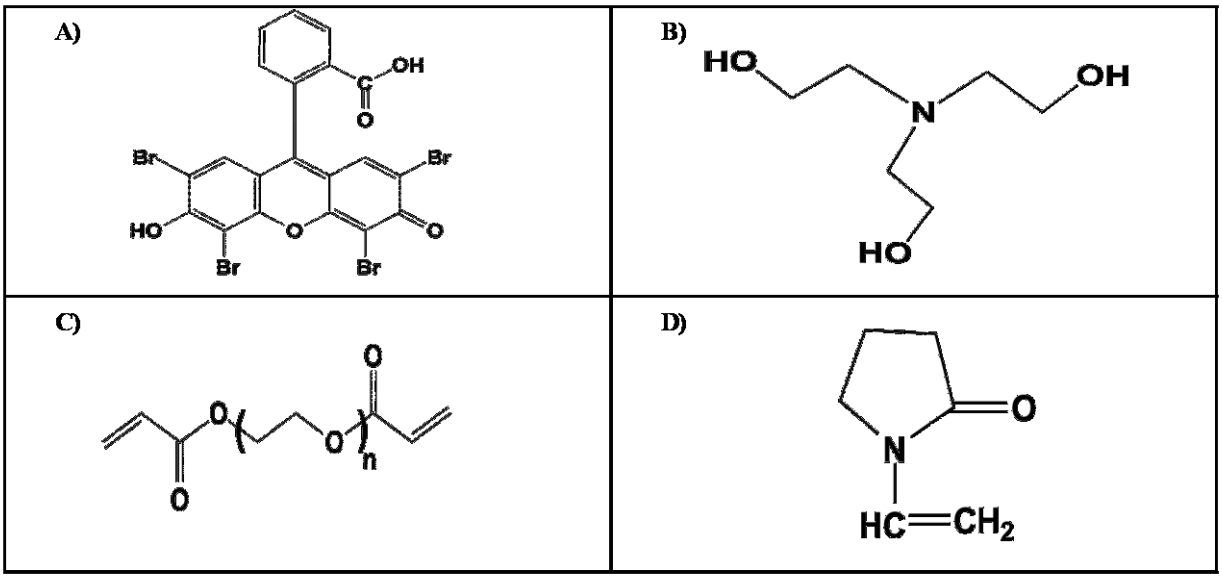

Figure 2.6 – Chemical structures of photopolymerization elements: A) Eosin Y (Photoinitiator), B) Triethanolamine (Co-initiator), C) PEGDA (Monomer), D) 1-Vinyl 2-pyrrolidone (Accelerator and monomer)

This PEG hydrogel synthesis technique was employed on glass or silicon surface initially (figure 2.8). In this method, silicon or glass surface was functionalized with Aminopropyl-Triethoxysilane (APTES) via silanization reaction. After amine functionalized surface is prepared, EY was covalently bound on the surface using Woodward's Reagent K (WRK) chemistry.

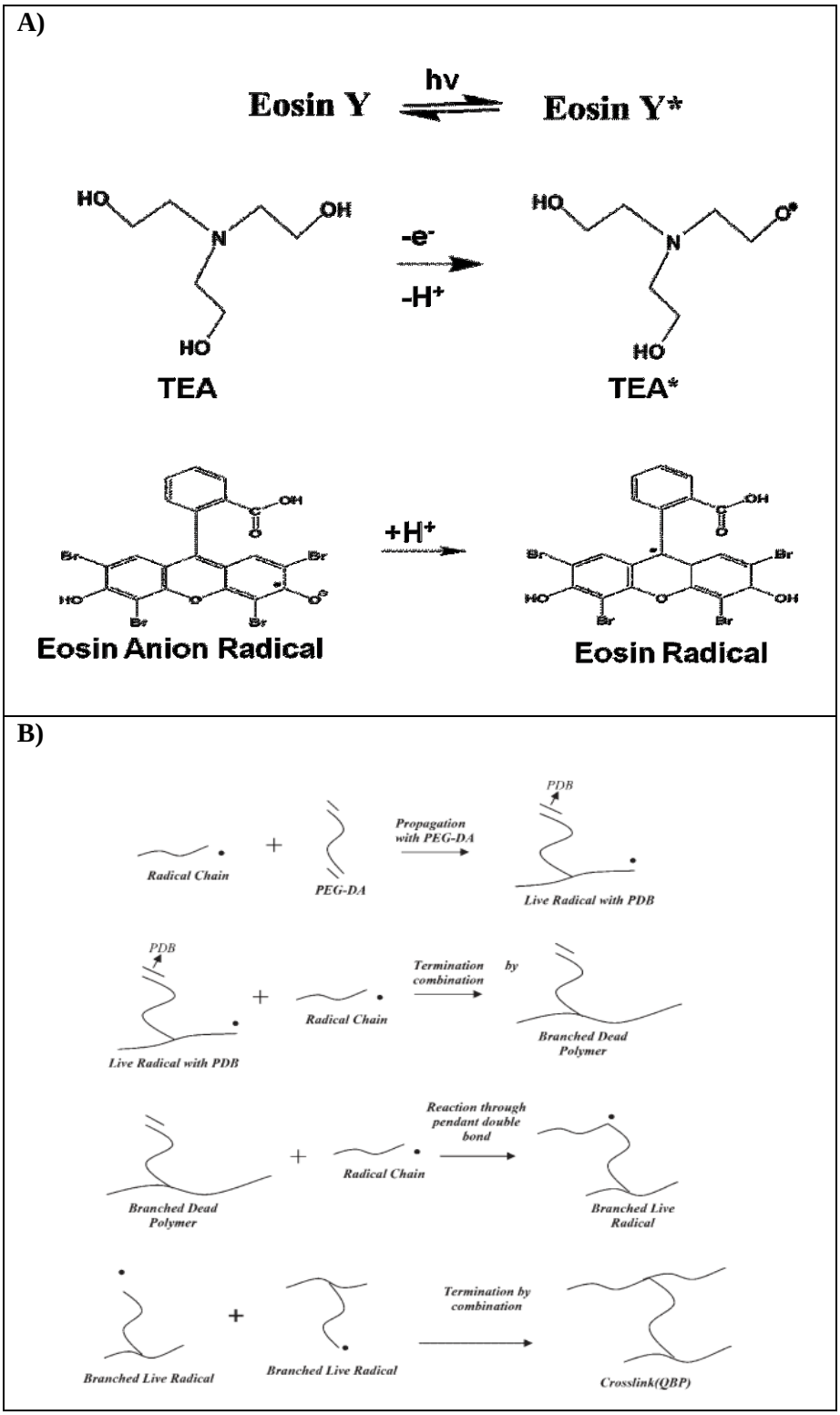

Figure 2.7 – A) Schematic illustration of photoinitiation process [3], B) Gel formation reaction of PEGDA [47]

After reaction, amide bond occurs between carboxyl group of EY and amine group of functional surface. Prepolymer solution which includes PEGDA, VP, TEA and PEG-peptide conjugate was poured on the EY-dyed surface. After illumination with green light, PEG hydrogel id synthesized on the substrate surface. PEG hydrogel synthesized in this study is a free radical polymerization reaction of PEGDA, VP and acryl-PEG-peptide.

This technique of producing covalently bound PEG hydrogel on surfaces via surface initiated photopolymerization is appropriate for surfaces that are functionalized with amine groups. In this thesis, our objective was to encapsulate cells or nanoparticles within biofunctional PEG hydrogel individually, while encapsulation of few islets or NPs in clusters is not completely avoidable due to the close proximity of islets or NPs within prepolymer solution. In the beginning, PEG hydrogel on the silicon surface was synthesized to be able to characterize swelling and thickness properties. Then, the system was adapted for encapsulation of pancreatic islets for treatment T1DM. Finally, encapsulation of MIONPs is achieved and has been demonstrated as promising to improve cellular uptake compared to uncoated MIONPs.

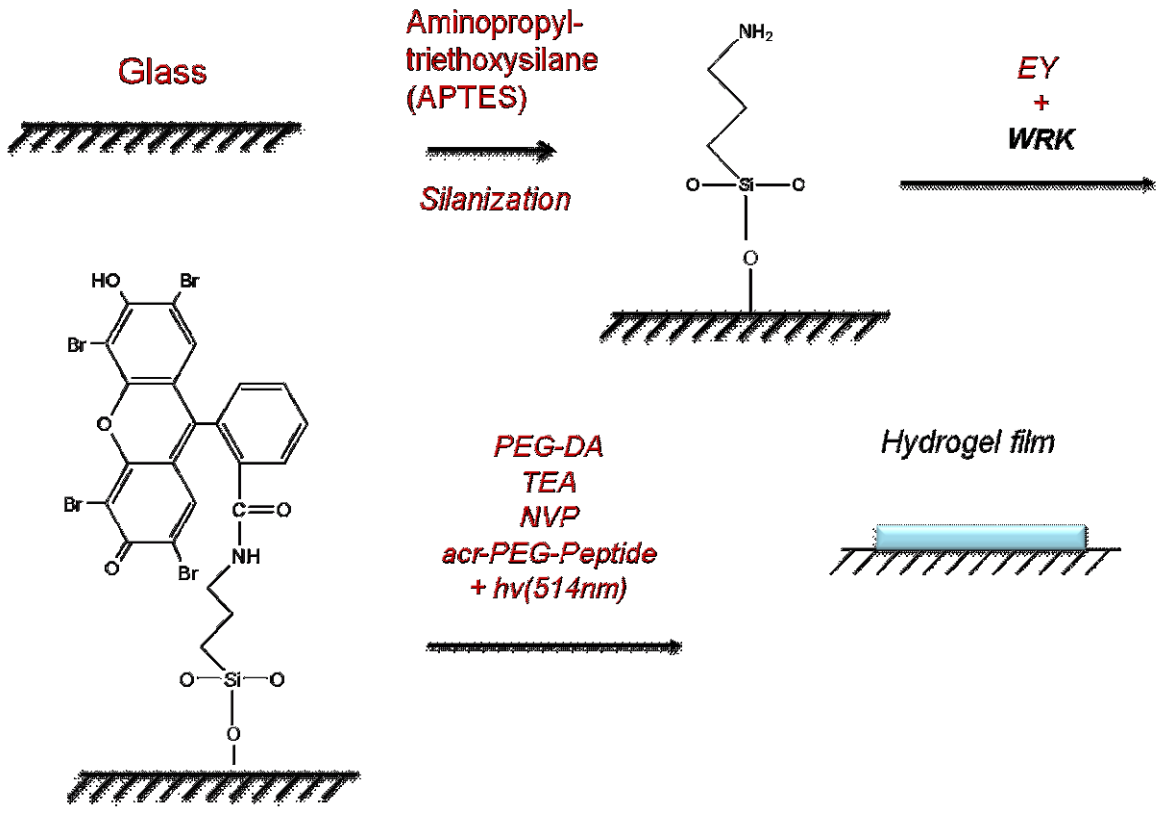

Figure 2.8 – PEG Hydrogel production on EY functionalized surface [3]

Chapter 3

EXPERIMENTAL SECTION

3.1. Experimental Part of the Pancreatic Islets Encapsulation

3.1.1. Materials

Sodium chloride (NaCl), Potassium chloride (KCl), Sodium bicarbonate ($NaHCO_3$), Calcium Chloride ($CaCl_2$), Magnesium Sulphate ($MgSO_4$), Potassium dihydrogen phosphate (KH_2PO_4), Streptavidin, bovine serum albumin (BSA), Fluorescein Diacetate (FDA), Propidium Iodide (PI), Eosin-Y, 1-vinyl-2-pyrrolidinone (VP), D-glucose, Acrylic acid N-hydroxysuccinimide ester (Acrylic acid NHS), were procured from Sigma. GLP-1 (7-37) and GLP-1 (9-37) were purchased from Elim Biopharmaceutical.). RPMI-1640 medium was purchased from Invitrogen Co. (Carlsbad, CA, USA). Phosphate Buffered Saline (PBS) was purchased from Gibco (CA). Fetal Bovine Serum (FBS) was obtained from Bioind.. Penicilin/streptomycin was purchased from Gibco. Poly(ethylene glycol)diacrylate (PEG DA, molecular weight: 3.4 kDa) was purchased from Laysan Bio (Arab, AL, USA). Acrylate PEG *N*-Hydroxysuccinimide (Acryl-PEG-NHS, MW: 3.4kDa) was purchased from Nektar. Triethanolamine (TEA) was purchased from Merck. 0.2uM Teflon Syringe Filter was obtained from Nalgene. Petri Dishes were purchased from Nunc. Dialysis cassettes were purchased from Pierce. Pancreatic Rat Isles were isolated and given by Istanbul University Experimental Medical Research Institute (DETAE). Cell-Titer-GLO Luminescent Viability Assay Kit was obtained from Promega. 96-well cell culture plate and 6-well cell culture plate were purchased from Greiner Bio-One. 96-well LUMITRAC™ 600 white immunology plate was obtained from USA Scientific. Rat Insulin Enzyme-Linked Immunosorbent Assay kit was purchased from Mercodia.

3.1.2. Methods

3.1.2.1. Production and Physical Characterization of Biofunctional PEG Hydrogel

3.1.2.1.1. Synthesis of Acrl-PEG-GLP-1 Conjugates

In this work, in order to synthesize biofunctional PEG hydrogel, glucagon-like peptide-1 (GLP-1(7-37), MW: 3356 Da; GLP-1(9-37), MW:3148 Da) were conjugated to monoacrylated PEG-NHS(MW:3400) with a molar ratio of 2 and allowed to react for 2 hours, in 50mM $NaHCO_3$, at a pH of 8.2 and at RT (figure 3.1). The reaction products were dialysed (MW cut off: 3500 Da) in order to remove unreacted reactants and premature oligomers. Concentration of GLP-1 in the PEG conjugates was measured by NanoDrop 1000 spectrophotometer (Thermo Scientific). The structure of GLP-1 (7-37), GLP-1 (9-37) and acrl-PEG-GLP-1 conjugates were verified by Fourier transform infra red (FTIR) spectroscopy (Thermo Scientific, Nicolet iS10 FT-IR spectrometer)

3.1.2.1.2. Determination of Swelling Raito of PEG-Peptide Conjugate Functionalized PEG Hydrogel

Petri Dishes (Polystyrene, 35mm diameter) were cleaned and treated with 1 mg /1 mL BSA at RT during 1 h. After washing, 1mL of 5 mM EY solution was poured on the Petri Dishes and incubated about 15 min to adsorb EY physically onto the surface (figure 3.2-A). Prepolymer solutions consisted of 25% PEG-DA, 225 mM TEA, $1.48x10^{-2}$ mM PEG-GLP-1 conjugate and VP concentrations of 19, 37, 74, 148, 592 mM were prepared. In order to investigate the effect of VP concentration to swelling property of PEG hydrogels, 2 mL of each of these solutions were placed onto EY adsorbed polystyrene surfaces. The substrates was illuminated via green light (λ: 514 nm, Power=5.1mW/cm^2) using Argon ion laser (Coherent, Innova 70C) during 150 sec. After synthesis, PEG hydrogels were transferred into PBS solution and incubated during 48 h in order to allow for its swelling, and gravimetric measurements were recorded until constant swelling was obtained. Swollen PEG hydrogels were weighed and percentage of swelling of each PEG hydrogels was calculated using the following equation

$$\% \text{ Swelling} = \frac{Wsf - Wd}{Wsi} \quad (3.1)$$

In previous equation, W_{si}, W_{sf} and W_d symbolize the initial weight of swollen hydrogel, final weight of swollen hydrogel and weight of dried hydrogel, respectively. The swelling ratio means that the fractional raise in the weight of the hydrogel as a result of water absorption [9].

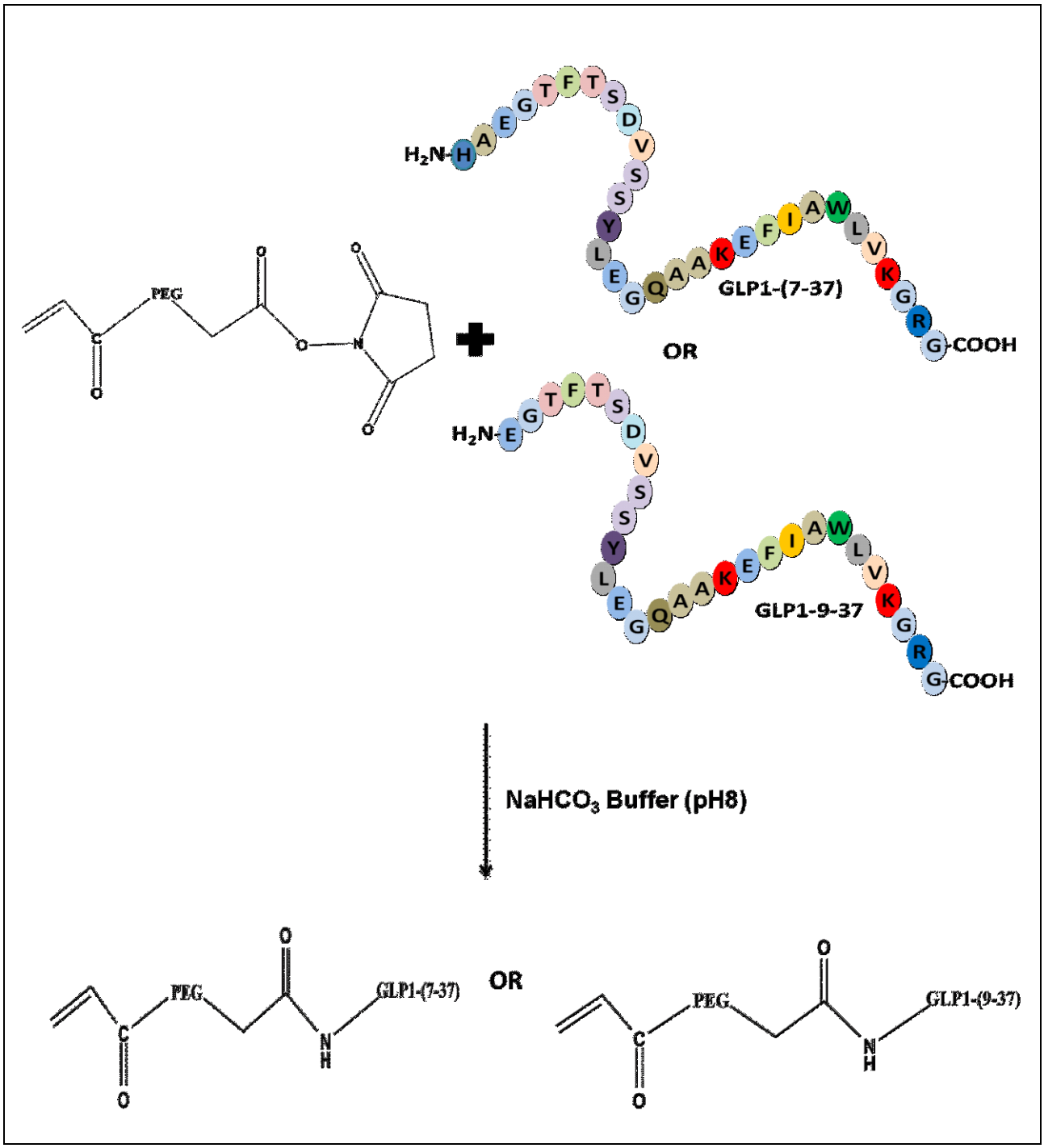

Figure 3.1 – Schematic illustration of acryl-PEG-GLP-1 conjugate synthesis

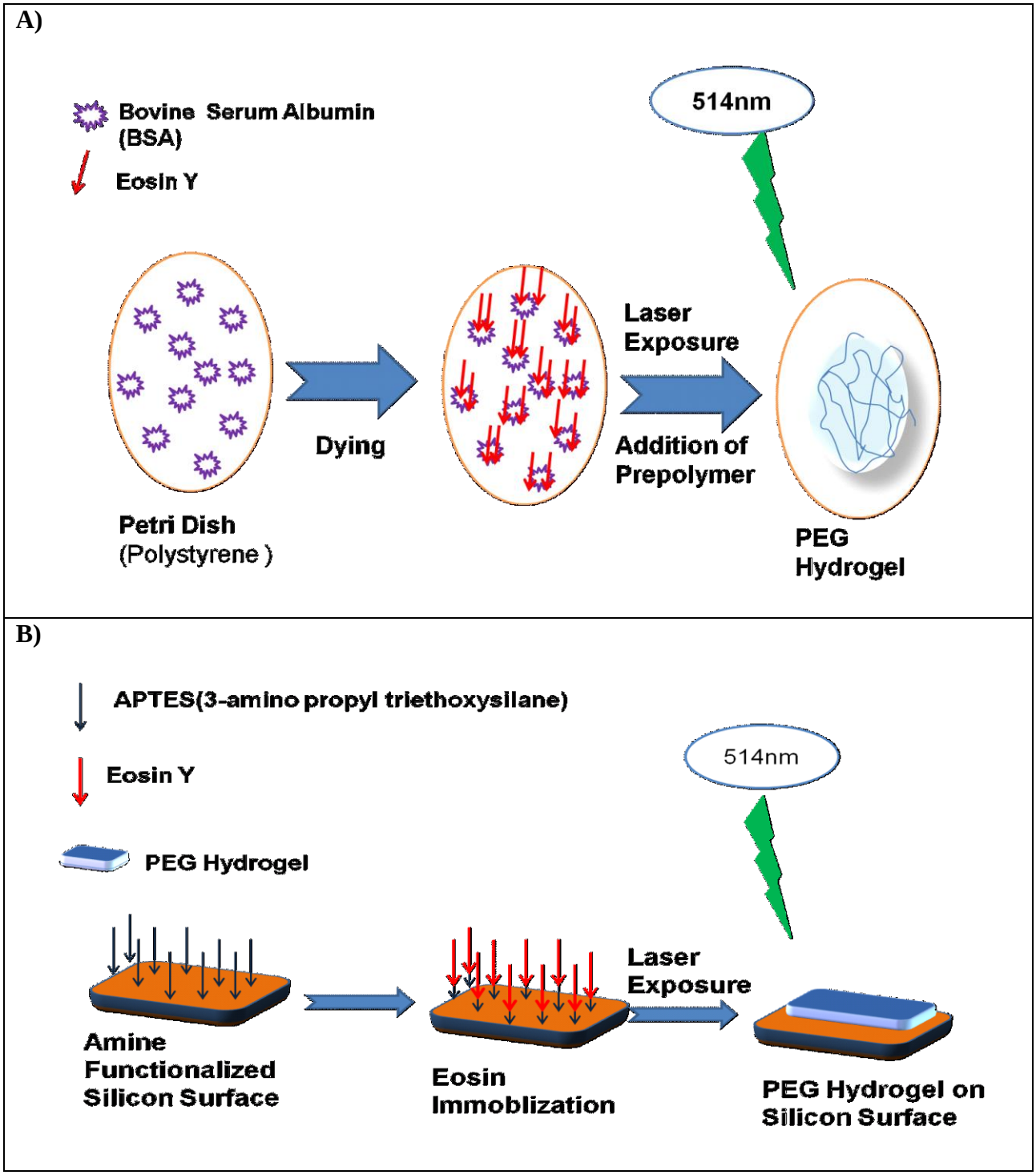

Figure 3.2 – PEG hydrogel production methods: A) For swelling characterization; B) For thickness measurement

3.1.2.1.3. Thickness Measurement PEG-Peptide Conjugate Functionalized PEG Hydrogel

Silicon wafers (100) were cut as 1(width)-2(length) cm manually in a dust-free environment. They were treated with piranha solution ((7/3)(v/v) H_2SO_4/H_2O_2) during overnight. Amine functionalized surfaces of silicones were prepared with 10%(v/v) APTES (3-aminopropil triethoxylane silane) in toluene solution under N_2 atmosphere. The samples were incubated at room temperature for 2 h. The modified substrates were washed 5 times with toluene in order to remove unbound deposited materials. Finally, substrates were rinsed with ethanol, water and ethanol again and finally dried with nitrogen gas. To prepare EY bound surfaces, each substrates were treated with 0.25 mM EY + 0.1 M WRK mixture for 30 min. After this step, all EY bound surfaces were washed with dH_2O and dried with N_2. Prepolymer solutions consisted of 15 % and 25% PEG-DA, 225 mM TEA, $1.48x10^{-2}$ mM PEG-GLP-1 conjugate and VP concentrations of 37, 111, 185, 333 and 592 mM were prepared, separately. A 20µL aliquot of prepolymer solution was placed onto the initiator-immobilized silicon surface (figure 3.2-B). The substrate was illuminated with laser for 150 sec (λ: 514 nm). Hence, at standard formulation (25% PEG-DA, 225 mM TEA, $1.48x10^{-2}$ mM PEG-GLP-1 conjugate and 37 mM VP), illumination time effects on the thickness of the PEG hydrogel was investigated from 20 to 180 sec. After the formation of the gel, the samples were broken in the middle and the height of the cross section of PEG hydrogel on silicon surface at eight different points were measured via Motic optical microscope as shown si figure 3.3. Finally, the images were processed via Motic Images Plus 2.0 program to thickness values.

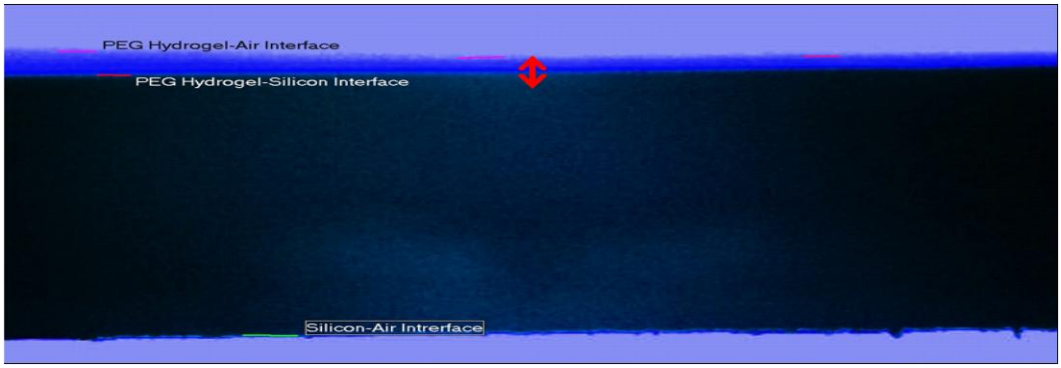

Figure 3.3 – Thickness measurement method of PEG hydrogel on the silicon surface via optical microscopy

3.1.2.2. Encapsulation of Pancreatic Islets within Biofunctional PEG Hydrogel

After the physical characterization of PEG hydrogels in terms of swelling and thickness, PEG hydrogel production model was adopted to encapsulate pancreatic islets. Rat islets were incubated with 5mM EY solution in PBS for 5 min. After washing of excess EY, stained islets were suspended in prepolymer solution (25 % PEGDA-3400, 225mM TEA, 37mM VP in PBS at pH 8) with or without GLP-1 conjugate (1.48x10-2 mM). Suspended islets were illuminated to coat them into biofunctional semi-permeable PEG hydrogel barrier (Laser Exposure Time: 150 sec; Laser Flux=2.5mW/cm^2). Then encapsulated islets were immediately washed with PBS. After washing, they were transferred into RPMI medium and incubated 24 h for further characterization. In order to investigate the effect of polymerization technique on islet cell viability, islets were encapsulated via surface initiated polymerization and bulk polymerization separately, and characterized for viability. In this procedure, instead of staining islets with EY, 50 μL of 5 mM EY was mixed with 1mL of prepolymer solution. Next, 20 pieces of islets were transferred into the prepolymer solution with EY, and the suspension was illuminated via green light using the same laser flux used for surface initiated techniques.

3.1.2.3. Investigation of Metabolic Activity of Encapsulated Islets

The metabolic activity of the encapsulated islets was measured via CellTiter-Glo assay which measures the amount of ATP in living cells. After 48 hours incubation of islets in RPMI medium, 20 islets from each group were transferred into 300 μL of fresh RPMI and CellTiter-Glo reagent mixture (Volume ratio: 1:1) separately. Next, they were cultured at RT for 1 hour on the orbital shaker. After the incubation, 200 μl of each sample were relocated into 96-well LUMITRAC™ 600 white immunology plate. In order to measure luminescence, the plate was read via The Fluoroskan Ascent FL (Thermo Scientific).

3.1.2.4. Investigation of Islet Function *in vitro* in terms of Insulin Secretion

In this assay, the naked and encapsulated islets were challenged with alternating concentration of glucose solutions dynamically by Biorep Perfusion Machine for 80 min (figure 3.4). Naked islets, PEG hydrogel encapsulated islets and biofunctional PEG hydrogel encapsulated islets were placed into the perifusion chambers seperately.

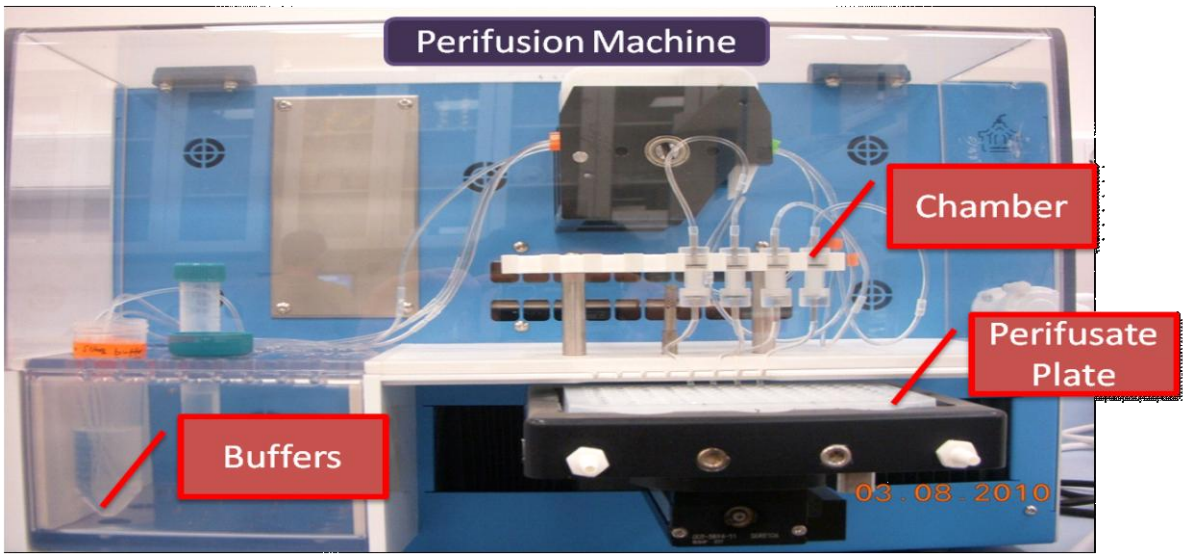

Figure 3.4 – Perifusion machine

A low pulsatility peristaltic pump drived perifusion buffers through the chambers containing 20 islets immobilized in Bio-Gel P-4 Gel (BioRad) with 100 µl/min rate. Glucose concentration was adjusted to 3.3 mM for a low glucose buffer, and 16.7 mM for a high glucose buffer (Table 3.1). Islets were exposed to low glucose buffer for 20 min after 20 min equilibration period with low glucose buffer. Then, they were treated with high glucose buffer for 20 min. Next, a washout perifusion with the low glucose buffer was carried out for 20 min. Finally, the islets were perifused with KCl buffer in order to release all insulin in the islet granules. The perifusates was collected every minute in a multiwell plate. The perifusion assay was applied at 37°C. The perifusate in the collecting plate was kept at <4°C. All perifusate samples obtained throughout the perifusion assay were stored at -20°C.

Table 3.1 – Ingredients of perifusion assay buffers

		Perifusion Buffers		
		Low Glucose	**High Glucose**	**KCl**
Material	**NaCl**	125 mM	125 mM	125 mM
	KCl	5.9 mM	5.9 mM	5.9 mM
	$CaCl_2$	2.56 mM	2.56 mM	2.56 mM
	$MgCl_2$	1 mM	1 mM	1 mM
	HEPES	25 mM	25 mM	25 mM
	BSA	0.10%	0.10%	0.10%
	D-glucose	3.3 mM	16.7 mM	0 mM

Finally, the amount of secreted insulin by encapsulated islets was monitored by Mercodia Rat Insulin Enzyme-Linked Immunosorbent Assay (ELISA) using ELISA reader (Biotek).

3.2. Experimental Part of the MIONP Encapsulation

3.2.1. Materials

3-(aminopropyl) trimethoxysilane–tetramethoxysilane (APTMS) coated magnetic iron oxide nanoparticles were given by H.F Yagci Acar Laboratory at Koç University. Eosin Y (EY) (91%), 1-vinyl-2-pyrrolidinone (99 %), poly-(ethylene glycol) diacrylate (MW: 575Da), Woodward's reagent K (WRK) (2-ethyl-5-phenylisox-azolium-3′-sulfonate, 95%), Phosphate buffered saline (PBS) and Triton X-100 were purchased from Sigma. Triethanol-amine (TEA) (99.5%) sodium bicarbonate ($NaHCO_3$) and 37% formaldehyde were obtained from Merck. Hydrochloric acid (HCl) and Sodium Hydroxide (NaOH) were purchased from Riedel-de Haen. Amicon Ultra centrifugal filter device (NMWL: 3000) was obtained from Millipore. Short peptide arginine-glycine-aspartic acid-serine (RGDS) (MW: 433Da) was purchased from Elim Biopharmaceuticals. Acrylate PEG *N*-Hydroxysuccinimide (Acryl-PEG-NHS, MW: 3.4kDa) was purchased from Nektar. Dialysis cassette (MW cutoff: 3.5kDa) and bicinchoninic acid (BCA) Assay were purchased from Pierce. 0.2 μm Teflon Syringe Filter was obtained from Nalgene. Petri Dishes were purchased from Nunc. Dulbecco's Modified Eagle Medium (liquid, with 4.5 g⁄L D-glucose and sodium pyruvate) (DMEM), L-Glutamine, penicilin/streptomycin (pen-strep) was purchased from Invitrogen. Fetal Bovine Serum (FBS) was obtained from Bioind. Trypsin-EDTA was purchased from Genlantis. Cell-Titer-GLO Luminescent Viability Assay Kit was obtained from Promega. 96-well cell culture plate and 6-well cell culture plate were purchased from Greiner Bio-One. 96-well LUMITRAC™ 600 white immunology plate was obtained from USA Scientific. Microscopy slide was purchased from Fisher Scientific. Cover slide was obtained from Isolab. Potassium ferrocyanide was purchased from Labkim.

3.2.2. Methods

3.2.2.1. Eosin Y Binding on the Surface of MIONPs

A 4 mM EY solution in dH_20 and a 20 mM WRK solution in 0.1 M NaOH were prepared and the solutions were adjusted to pH 9. Equal volumes of both EY and WRK solution were mixed and reacted for 30 min. Then, an equal volume of 40 mg/mL APTMS coated MIONP (with 20 mM amine group) solution in dH_2O was reacted with prepared EY -WRK mixture overnight at

RT in order to form amide bond between carboxylic group of EY and amine group of APTMS coated MIONPs (pH 9) (figure 3.5). After this, reaction mixture was washed via Amicon Ultra centrifugal filter device so that unbound EY, WRK residue and other ions were removed. EY content of the product was characterized via Nanodrop 1000 spectrophotometer (Thermo Scientific). Furthermore, the binding of EY to APTMS coated MIONP was confirmed by UV-VIS spectrophotometer (PG Instruments T80 Plus) and Fourier transform infra red (FT-IR) spectroscopy (Thermo Scientific, Nicolet iS10 FT-IR spectrometer).

3.2.2.2. Synthesis of Acryl-PEG-RGDS Conjugate

To functionalize MIONPs for subsequent delivery and cellular uptake, we synthesized PEG-RGDS conjugate via *N*-Hydroxysuccinimide chemistry. 1 mg/ml of short peptide RGDS and 10 mg/ml of Acryl-PEG-NHS were separately prepared in 50 mM $NaHCO_3$ at pH 8.2. Acryl-PEG-NHS solution was added by drop wise to the peptide solution until the mole ratio of Acryl-PEG-NHS to the peptide was 1:1. The conjugation reaction was carried out for 2 h at RT and by rocking (figure 3.6-A). After the reaction, the reaction mixture was dialyzed against to dH_2O in order to eliminate unreacted Acryl-PEG-NHS and peptide.

The synthesized Acryl-PEG-RGDS conjugate was characterized by Nanodrop 1000 spectrophotometer (Thermo Scientific) using BCA Assay. The structure of acryl-PEG-RGDS conjugate was confirmed by Fourier transform infra red (FTIR) spectroscopy (Thermo Scientific, Nicolet iS10 FT-IR spectrometer).

3.2.2.3. Prepolymer Solution Preparation

The prepolymer solution containing 6.25 % PEGDA (w/v) (MW:575 Da), 141 mM TEA (Co-initiator) and 24 mM VP (accelerator) was prepared in dH_2O to use for the encapsulation of MIONPs within biofunctional PEG hydrogel. In order to produce biofunctional PEG hydrogel coating over MIONPs, acryl-PEG-RGDS was added into prepolymer solution at final concentration of $1.48*10^{-2}$ mM.

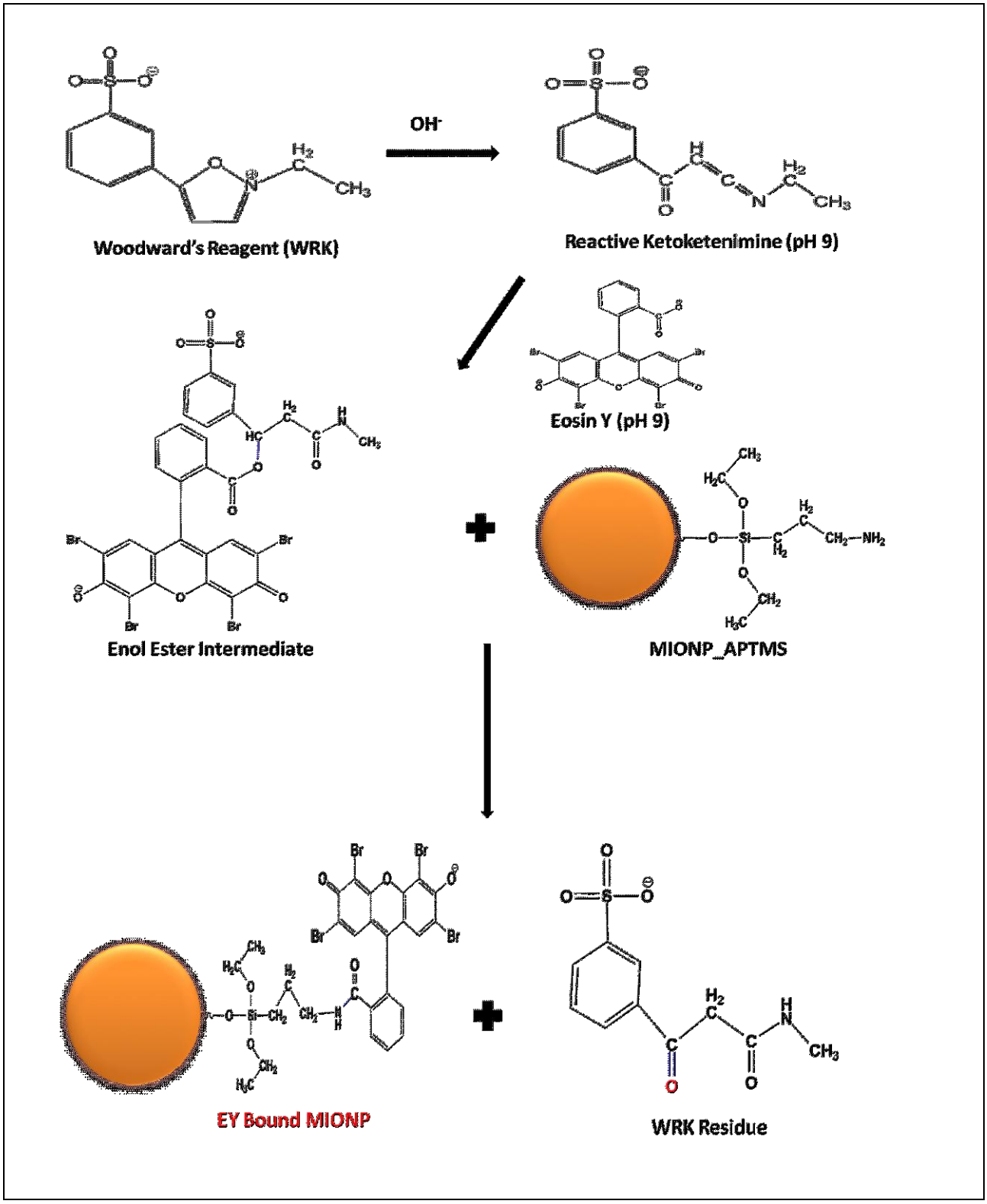

Figure 3.5 – EY binding on to the surface of MIONP

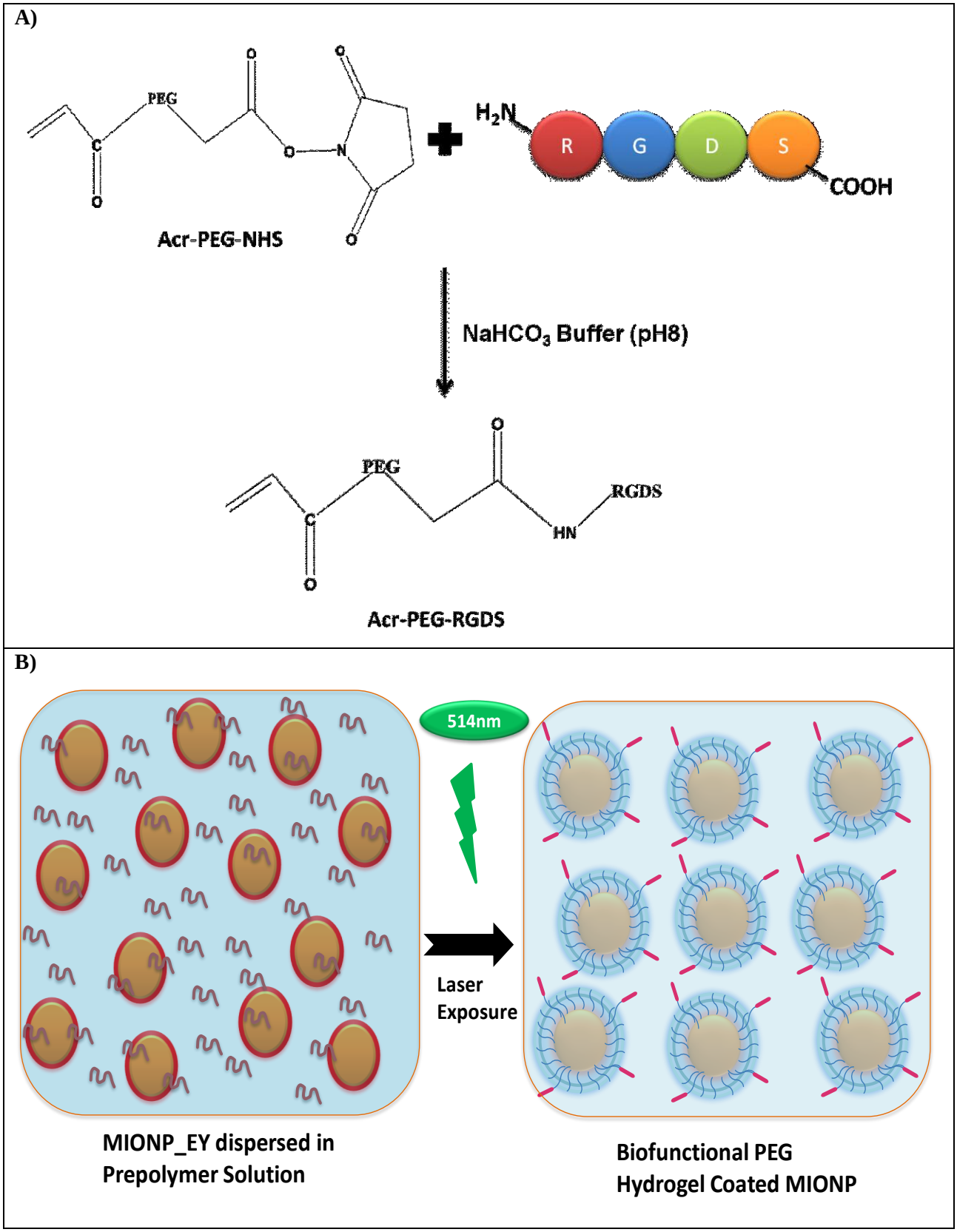

Figure 3.6 – **A)** PEG-Peptide conjugate synthesis, **B)** Encapsulation method of MIONPs

3.2.2.4. Encapsulation of MIONPs within Biofunctional PEG Hydrogel

After covalent binding of EY onto the surface of the MIONPs, 0.5mg/ml modified MIONPs solution was mixed with the prepolymer solution (Final Concentrations: 5% PEGDA-575, 19mM VP, 113 mM TEA, 1.48*10-2 mM acryl-PEG(3400)-RGDS, 0.1mg/ml MIONP). The solution was adjusted to pH 8 using HCl. Next, the mixture was illuminated via green light (λ: 514 nm, P: 2.5 mW/cm^2) using Argon ion laser (Coherent, Innova 70C) at varied time interval (20, 30, 60 sec.). PEG hydrogel could coat the MIONPs as seen in figure 3.6-B.

3.2.2.5. Structural, Chemical and Physicochemical Characterization of MIONPs

EY-bound and PEG hydrogel encapsulated MIONPs (EMIONPs) were characterized in terms of structure, size, stability and morphology. Analysis of structural changes in terms of chemical bonding was assessed via FT-IR. Also, photo-bleaching of EY dye was shown via UV-Vis spectrophotometer after photopolymerization reaction. Hydrodynamic particle size of EMIONPs was determined via dynamic light scattering (DLS) (Malvern). The colloidal stability was characterized through zeta potential of EMIONPs using ZetaPals (Brookhaven). The morphology of the EMIONPs was analyzed via Solver S47 (NT-MDT) scanning probe microscopy platform in intermittent atomic force microscope (AFM) mode.

3.2.2.6. Toxicity Analysis of MIONPs

After obtaining desired EMIONPs for *in vivo* study, cytotoxicity analysis was examined via exposing HeLa cells with varied EMIONPs. HeLa cell lines were seeded at 5x10^4 cells/mL in 96-well plate and cultured 24 h and 48 h in DMEM (pH 7.4, with 10% FBS, 1% Pen-Strep and L-Glutamine). Suspensions with APTMS coated MIONPs, EY-bound MIONPs, PEG hydrogel coated MIONPs and biofunctional PEG hydrogel coated MIONPs were added into HeLa cells culture medium in triplicate. After 24 and 48 h incubation, Cell-Titer-GLO Luminescent Viability Assay was carried out using Fluoroskan Ascent Luminescent Reader (Thermoscientific).

3.2.2.7. Cellular Uptake of MIONPs

3.2.2.7.1. Prussian Blue Staining

Cellular uptakes of APTMS, PEG hydrogel and biofunctional PEG hydrogel coated MIONPs were compared via Prussian blue staining. For this purpose, $5x10^6$ HeLa cells were cultivated for 48 h in 6-well plates on glass coverslips. After HeLa cells covered the surface of the slides, uncoated and coated 100 μL 0.5 mg/mL of MIONPs were added into each well. After 24 h incubation, HeLa cells on the coverslides were washed thrice with PBS and fixed with 4% formaldehyde for 20 min at RT. After fixation, the cells were treated with 0.1 % Triton X-100 for 5 min and washed with PBS. This step was repeated four times. For Prussian blue staining, fixed HeLa cells were incubated with 5% potassium ferrocyanide in 10% HCl during 15 min. Finally, stained cells were observed via optical microscopy equipped camera (Motic).

3.2.2.7.2. Determination of the Intracellular Iron Content

Cellular uptakes of the APTMS, PEG hydrogel coated and biofunctional PEG hydrogel coated MIONPs were determined qualitatively via ICP-OES. HeLa Cells were grown in D-MEM into 24-well plate (10^5 cells in 1mL of medium) (1mL of cell culture was added into each well). After 24 h incubation, APTMS, PEG hydrogel coated and biofunctional PEG hydrogel coated MIONPs were added into medium at 0.1mg/mL concentration. In control culture, the cells were placed in 1ml medium without NPs at the same cell density. After 24 h treatment with the NPs, cells were washed with PBS three times. Cells were detached via trypsin-EDTA solution (0.25 mL in each well). Detached cells were incubated in a mixture of 0.25 ml 65% nitric acid and 0.25 mL 30% hydrogen peroxide about 24 h at 90°C. Finally, ICP analysis was performed for all samples.

3.3. Statistical Analysis

ANOVA technique was applied for statistical analysis. All data was represented as mean ± standard deviation of mean. $P < 0.05$ was thought to be statistically significant.

Chapter 4

RESULTS AND DISCUSSION

4.1. Characterization of Swelling and Thickness Properties of Biofunctional PEG hydrogel

A variety of approaches for microencapsulation of islets have been advanced using synthetic and natural polymers based on PEG hydrogels [5], alginate[48], or living cells [49] to hinder transplanted islets from host immune attack. Most of microencapsulation techniques suffer from a suitable transplant volume, essential metabolites and diffusion efficiency, as well as immunosuppressive drug free curing [50]. In order to address limitations associated with other techniques of encapsulation; surface initiated photopolymerization have been investigated in this study to encapsulate islets within biofunctional PEG hydrogel. Herein, our *in vitro* results showed that this technique does not compromise islet viability and functionality and further enhance islet encapsulation efficiency compared to existing techniques of islet encapsulation.

In this study, PEG-peptide conjugates were synthesized in order to functionalize PEG hydrogel coating on islet surface. Peptide weight percentage of acryl-PEG-GLP-1 conjugates were confirmed using UV-Vis spectrophotometer (Nanodrop) measured at 280 nm. The GLP-1 content of the acryl-PEG-GLP1-(7-37) conjugate product was estimated as 44% (by weight). Theoretically, the conjugate product of the acryl-PEG-GLP1-(7-37) composed of 89 % acryl-PEG-GLP1-(7-37) by weight. The GLP-1 content of the acryl-PEG-GLP1-(9-37) conjugate product was estimated as 46% (by weight). Theoretically, the conjugate product of acryl-PEG-GLP1-(9-37) composed of 95 % acryl-PEG-GLP1-(9-37) by weight. The formation of the chemical bond between GLP-1 peptides and acryl-PEG was characterized via FT-IR analysis. In the FT-IR spectra, the carbonyl groups (C=O) in NHS ester exhibits two peaks at 1781cm^{-1} and 1820 cm^{-1} [51]. After the conjugation reaction, disappearance of these carbonyl bands points to that the NHS ester reacted with the amine groups in the GLP-1 peptide structure and new amide bonds were formed as seen at figure 4.1. The peak corresponding to the carbonyl group in acryl-

PEG-NHS was seen around 1740 cm^{-1}. After the conjugation reaction, amide I peak appeared at 1670cm^{-1} different from acryl-PEG-NHS. It could be concluded that the conjugation reactions between peptide and PEG were carried out successfully.

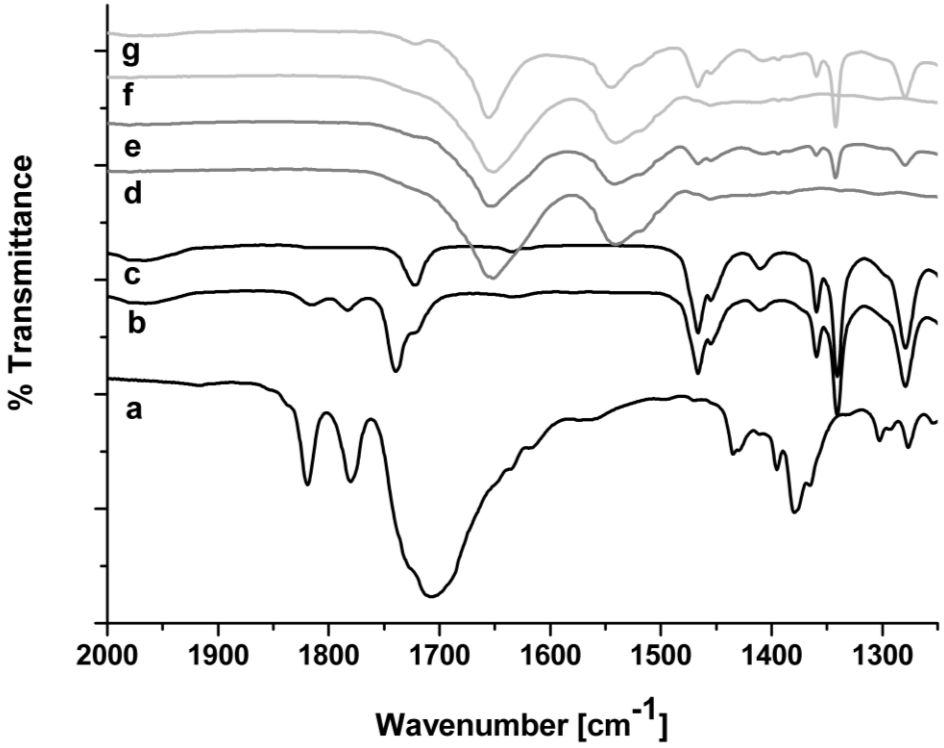

Figure 4.1 – FT-IR spectra of: a) Acrylic acid NHS, b) acryl-PEG-NHS, c) PEGDA, d) GLP-1 (7-37), e) acryl-PEG-GLP-1(7-37), f) GLP-1(9-37), g) acryl-PEG-GLP-1(9-37)

VP concentration of the prepolymer solution influences the gel thickness and encapsulation ability [5]. So, the effect of VP concentration on PEG hydrogel swelling and thickness has been investigated in this study. Swelling is an important property of hydrogels. High swelling means that water uptake capacity of hydrogel network is high, and hence denotes high solute permeability of hydrogel. [9]. Hydrogels have been synthesized with varying concentrations of VP monomer, and have been incubated at PBS solution. Next, gravimetric measurements have been carried out until constant weight of hydrogel is measured (figure 4.2). Increasing the VP concentration for standard conditions (25 % PEGDA-3400, 225mM TEA, 1.48 X 10^{-2} mM PEG-GLP-1) decreased the solution absorption ratios of the PEG hydrogel. It could be speculated that permeability of the PEG hydrogel with conjugate was very low at high VP concentrations because of the increasing the crosslink density. Since, VP works as an accelerator during

reaction; it propagates through the carbon-carbon double bonds of the acrylate end groups to form polyacrylate chains.

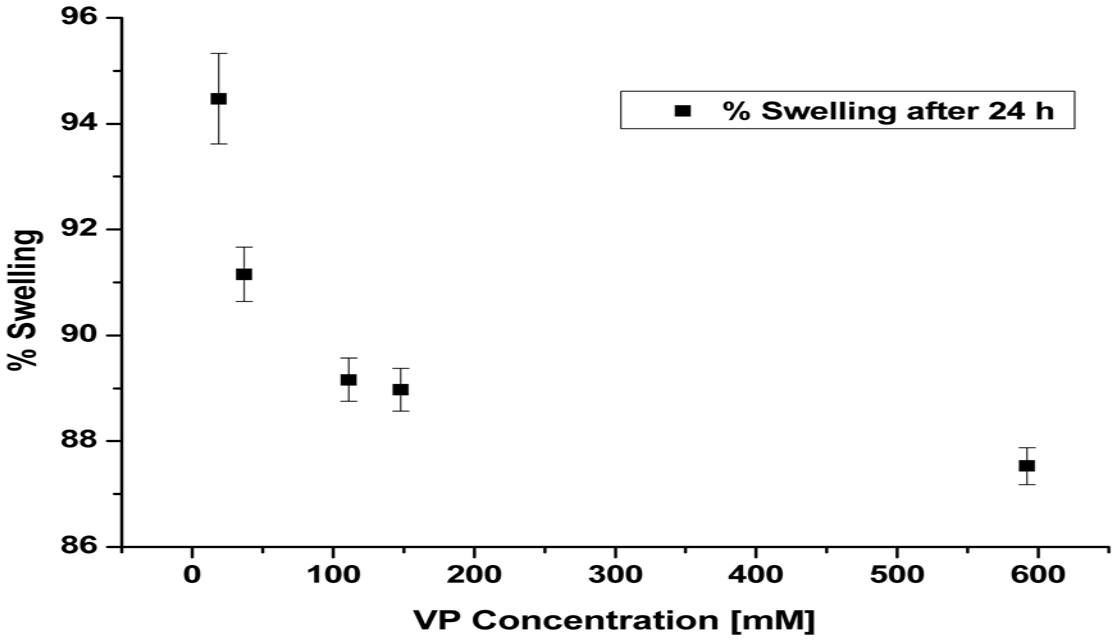

Figure 4.2 – Effect of VP concentration on swelling of biofunctional PEG hydrogels

Increasing VP concentration from 37 to 333 mM considerably increased the thickness of the PEG hydrogel with PEG-GLP-1 conjugate on the silicon surface for both cases of the 15 and 25 % PEGDA concentrations (figure 4.3). The thickness of the hydrogel membrane measured for the 15 % (w/v) PEGDA condition increases with the increment of VP concentration and reaches about 100 μm at 592 mM VP concentration. The PEG hydrogel thickness could reach about 100 μm at 185 mM VP concentration for 25 % (w/v) PEGDA concentration. It could be concluded that VP and PEGDA promote photopolymerization, and hence higher concentration any each monomer results in higher thicknesses. Furthermore, the effect of illumination time on the thickness of PEG hydrogel can be observed in figure 4.4, which demonstrated again higher thicknesses of the hydrogel with exposure time. These results suggest that it is possible to fine tune hydrogel thicknesses as a function of either monomer concentration or polymerization time. Based on these results, 37mM VP and 120 sec illumination time conditions were selected for the case of 25 % (w/v) PEGDA condition in order to produce 50 μm thick PEG hydrogel coating with low crosslink density around islets.

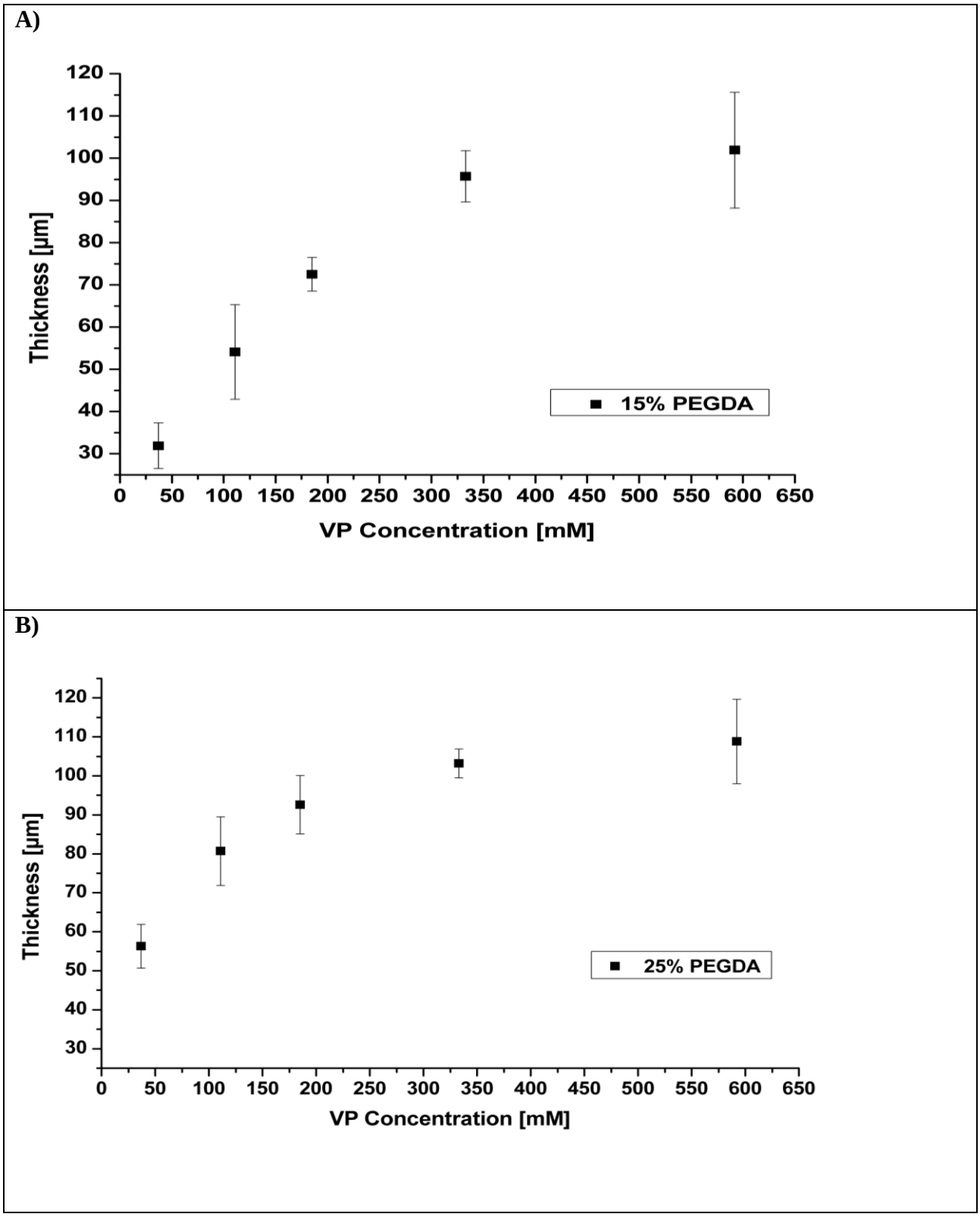

Figure 4.3 – The Thickness of biofunctionalized PEG hydrogel membrane versus VP concentration: A) 15 % PEGDA, B) 25 % PEGDA

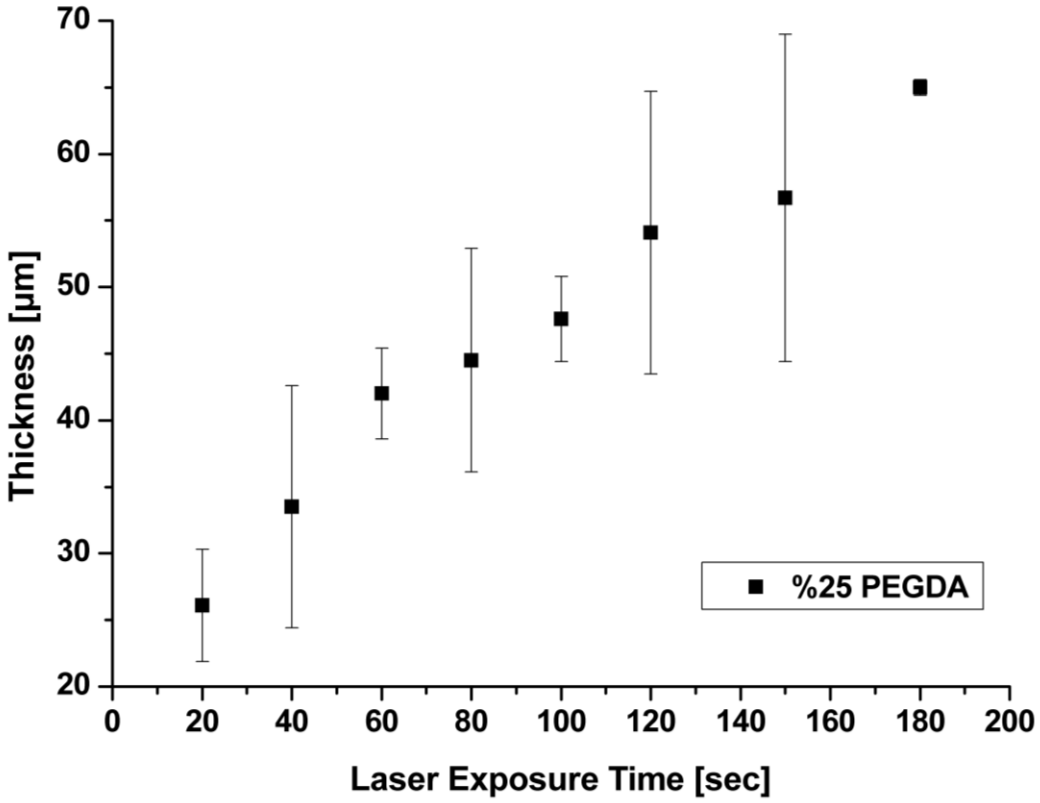

Figure 4.4 – Effect of illumination time on the thickness of PEG hydrogel

4.2. Microencapsulation of Pancreatic Islets within PEG Hydrogel

It is well established in the literature that the presence of specific biomolecules within 3-D microenvironment enhance cell migration, viability and function. Therefore, in this study GLP-1 has been exploited as an insulinotropic biomolecule, and covalently incorporated into the PEG hydrogel structure. As previously described, GLP-1 was bound to PEGMA covalently via NHS chemistry. During photopolymerization, GLP-1-PEGMA conjugate can attach the PEG network via acrylate group. GLP-1 immobilized PEG hydrogel coating can not only enhance viability and functionality of islets, but also reduce the number of islets desired to accomplish normoglycemia [9].

The application of biofunctional PEG hydrogel seems to be useful for enhancing islets viability and functionality after transplantation. The coating method that is employed in this study is based on cross-linking reaction of soluble PEGDA chains and GLP-1-PEGMA conjugate into

gel form as a barrier surrounding the islets. Since, EY (Photoinitiator) is physically adsorbed only islets surface, the photopolymerization of PEGDA occurs over the islet surface instead of formation bulk structure. In order to compare surface initiated method and bulk polymerization method, islets were also encapsulated into bulk PEG hydrogel (figure 4.5-D). It could be inferred from figure 4.5 that PEG hydrogel coating conformed the shape of the islets. Thickness of PEG hydrogel coating was about 30 µm. The surface initiated polymerization leads to dense variation of the hydrogel covering the islets. While, a more densely cross-linked hydrogel network produces near the islet surfaces, density of the cross-linking decreases at points further from islet surface.

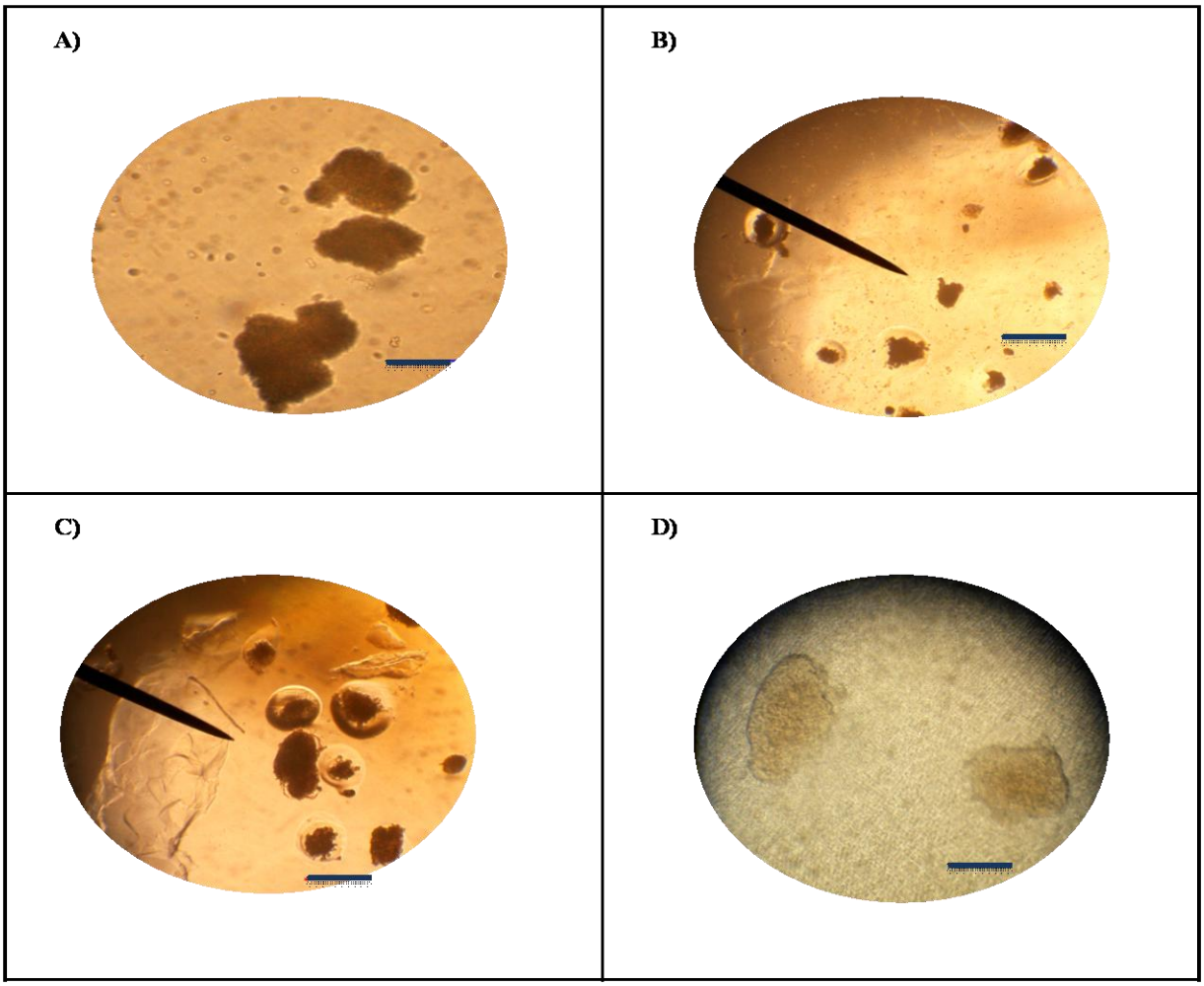

Figure 4.5 – Optical microscopy images of islets: A) Naked islets, B) PEG hydrogel encapsulated islets, C) Biofunctional PEG hydrogel encapsulated islets, D) Bulk PEG hydrogel encapsulated islets (Scale Bar length: 100 µm)

Figure 4.6 illustrates that GLP-1(7-37) immobilized PEG hydrogel could promote the long-term survival of the islets. Only PEG hydrogel coating and PEG hydrogel produced via bulk polymerization coating affected unfavorably the cellular metabolic activity in islets because 50 % diminish occurred in ATP production of islets when they compared with naked islets. It could be concluded from figure 4.6 that GLP-1 functionalized PEG hydrogel coating via surface initiated photopolymerization increases the metabolic activity about two more times excess when compared to naked islets.

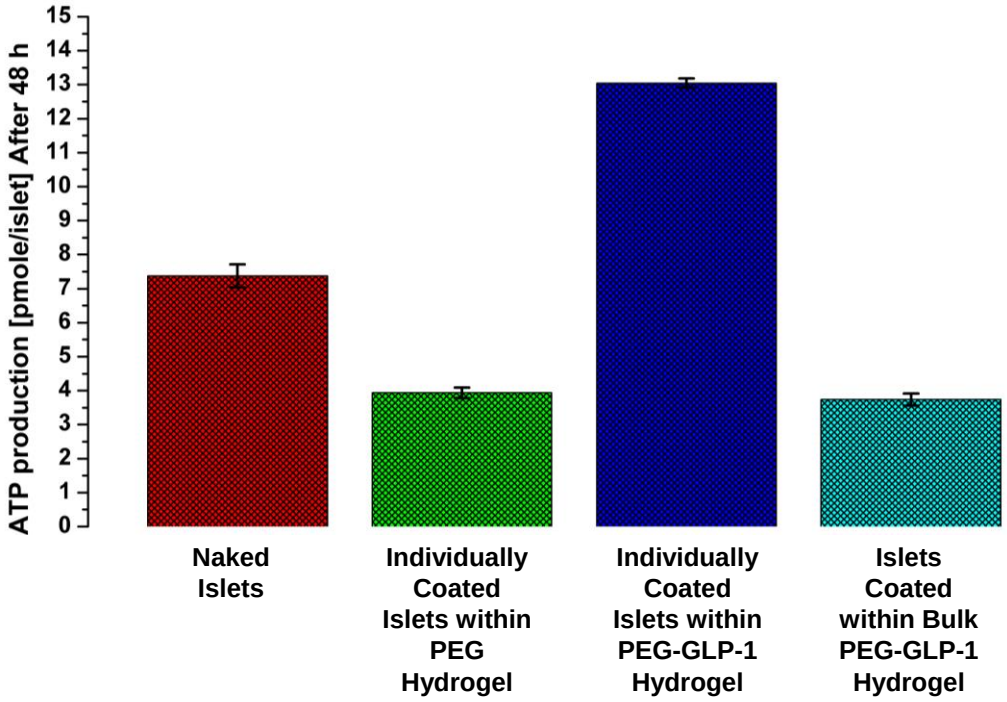

Figure 4.6 – Metabolic activity of encapsulated islets in terms of ATP production

In order to investigate the functionality of encapsulated islets, dynamic perifusion assay has been performed. This assay determines the time-dependent secreted insulin in responce to varying concentrations of glucose [33] for about 1 h. Figure 4.7 shows that islets in all three groups can respond to changes in glucose concentration, and secrete higher insulin at higher glucose levels. Bioactive GLP-1 (7-37) immobilized PEG hydrogel encapsulated islets demonstrated a considerably higher response in high glucose environment as expected. This is probably because GLP-1 (7-37) has interacted with its receptor on islet surface, and stimulated glucose dependent insulin secretion compared to the magnitude of insulin in other groups.

Immobilization of GLP-1 (7-37) into PEG hydrogel structure is promising approach, and may allow for reducing transplantation volume of encapsulated islets as a result of enhanced functionality.

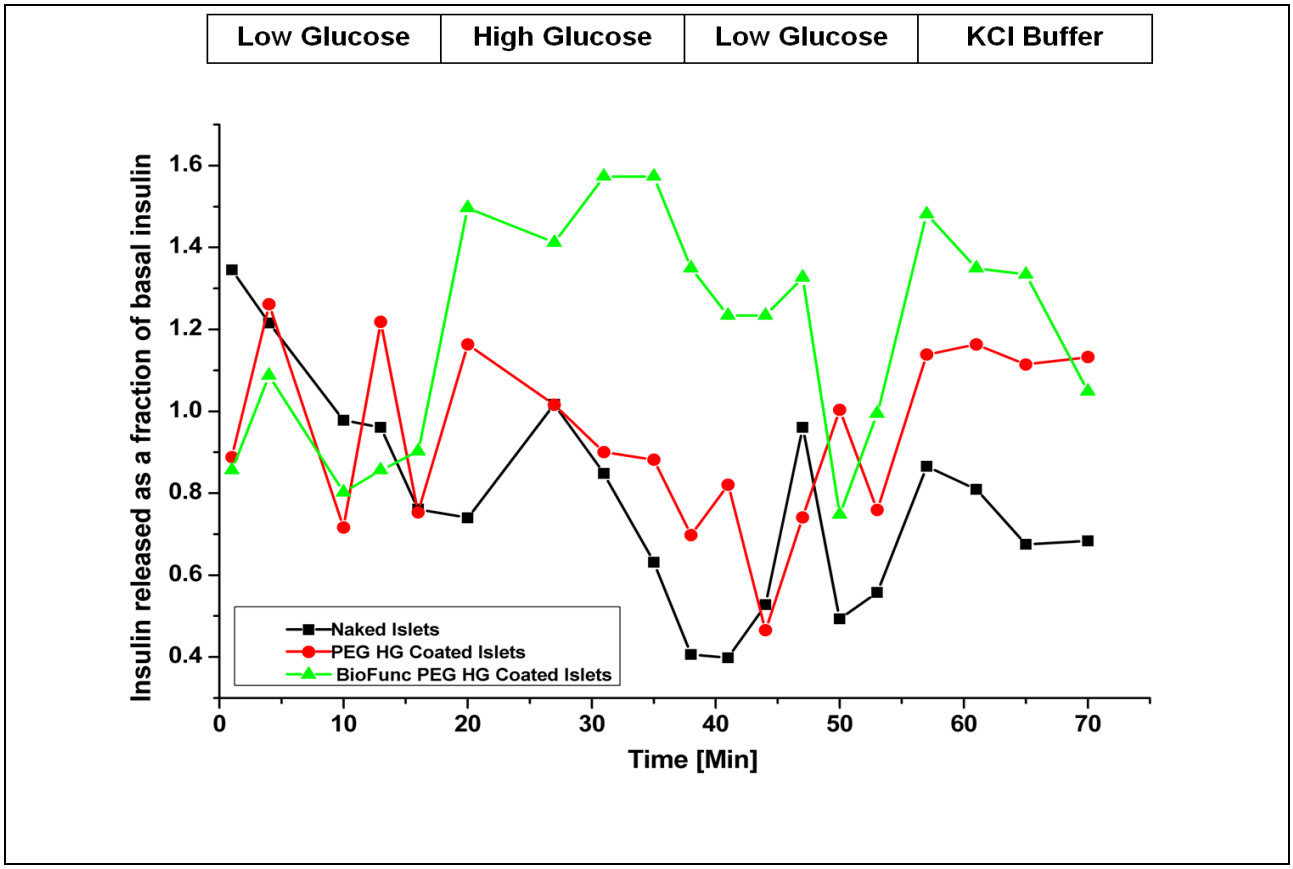

Figure 4.7 – Dynamic insulin response to glucose stimulation results of encapsulated islets

Biofunctional PEG hydrogel also suggests an optimal volume-to-surface ratio for rapid replace of hormones and nutrients. Furthermore, mild photopolymerization conditions used in this study provide elimination of cytotoxicity and loss of functionality. The size and mechanical characteristics of most of the existing microcapsules prevent the selection of the intra-portal vein of the liver as a transplantation site which has been selected as the ideal site with high oxygen and nutrient environment for islets [52]. The biofunctional PEG hydrogel system with bioactive cues allows transplantation into intra-portal vein with its smaller graft volume and higher insulin performance.

4.3. Encapsulation of MIONPs within Biofunctional PEG Hydrogel

4.3.1. Results

4.3.1.1. Absorption Spectral Analysis

UV-Vis spectra of APTMS coated MIONPs could be observed in figure 4.8-A. After EY binding on MIONPs, EY content of the product was determined using UV-Vis spectrophotometer measured at 537 nm (Light absorption maximum of EY is around 537 nm [53]). After the binding reaction, the product contained 12 % EY by weight. This content corresponded that efficiency of EY binding on MIONPs was 57 %.

The presence of acryl-PEG-RGDS conjugate was confirmed by BCA assay using UV-Vis spectrophotometer measured at 562 nm. The RGDS content of the acryl-PEG-RGDS conjugate product was estimated as 8 % (by weight). The conjugate product composed of 70 % acryl-PEG-RGDS.

4.3.1.2. FT-IR Spectral Studies

The binding of EY to APTMS coated MIONP was confirmed by FT-IR analysis. Figure 4.9-A shows the FT-IR spectra of APTMS coated MIONP and EY-bound MIONP. The FT-IR spectra of APTMS coated MIONP exhibited two peaks at 571 cm^{-1} and 590 cm^{-1} due to iron oxide skeleton [54-56]. The peaks at 919, 1215, 1328, 1388, 1505, 1617 and 2931 cm^{-1} were assigned to C-H out-of-plane bending, aliphatic C–N stretching, aliphatic C-O stretching, Si-CH_2 scissoring, C-H bending, NH_2 scissoring & N-H bending and CH_2 stretching, respectively [54, 57-58]. After EY binding these peaks were protected except the peak at 1505 cm^{-1}. The bands at 1456 cm^{-1} and 1541 cm^{-1} which corresponded aromatic C-C stretching and aromatic C=C stretching due to EY structure appeared after EY binding to MIONP. These new peaks overlapped C-H bending peak at 1505 cm^{-1}. The peaks at 3058 and 3352 cm^{-1} produced shoulder structure because of NH_2 stretching in the APTMS coated MIONP [58]. This shoulder structure disappeared mostly and one new peak at 3156 cm^{-1} which corresponded secondary amide N-H stretching appeared after the EY binding [58]. These two FT-IR spectra gave strong evidence about EY binding on MIONP covalently.

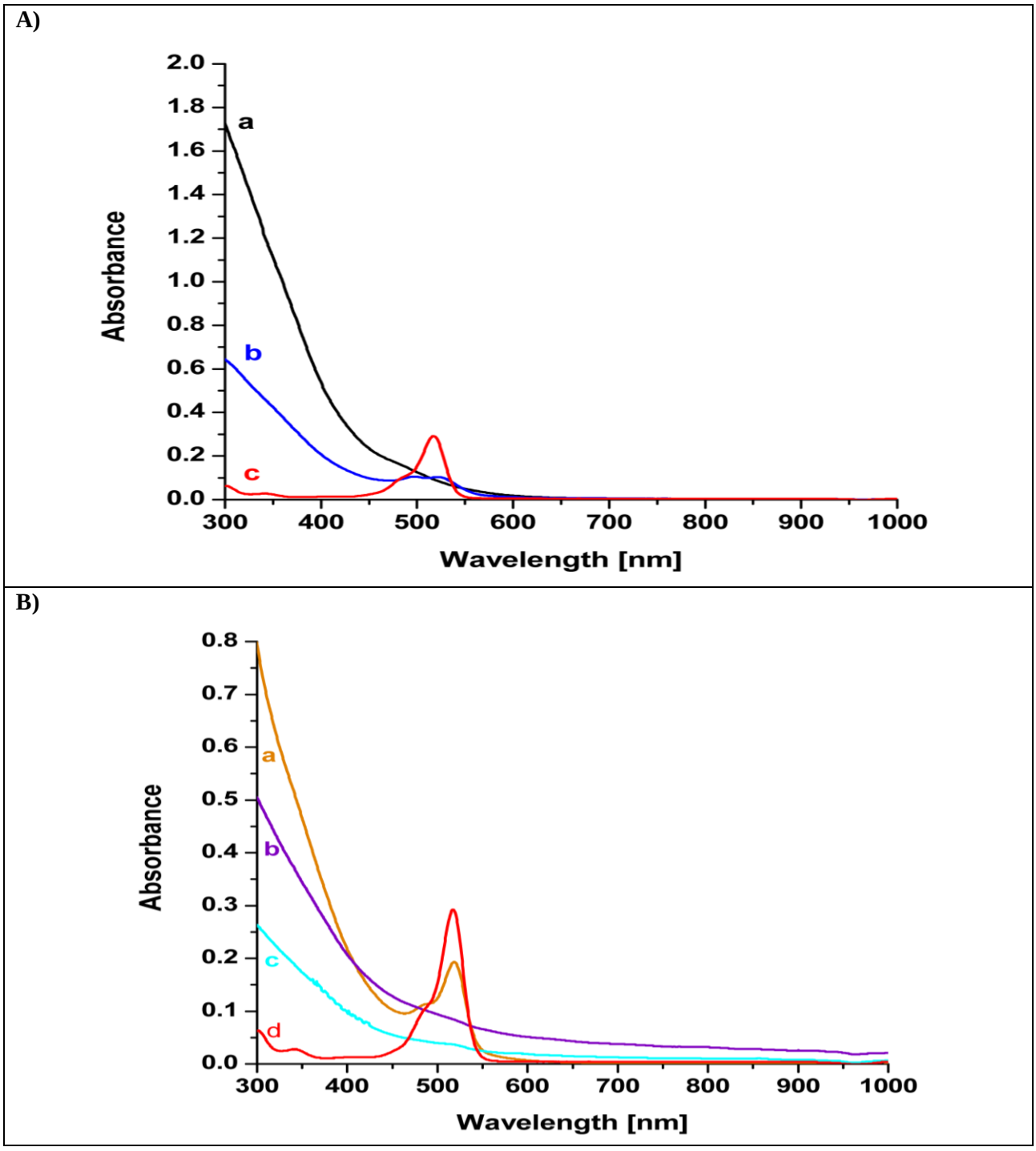

Figure 4.8 – **A)** UV-Vis spectra: a) APTMS-coated MIONPs, b) EY-bound MIONPs, c) EY dye; **B)** Photo-bleaching of EY dye after photopolymerization: a) EY-bound MIONPs in prepolymer solution before reaction, b) Encapsulated MIONPs within PEG hydrogel, c) Encapsulated MIONPs within PEG-RGDS bound PEG hydrogel, d) EY dye

In this study, PEG-peptide conjugate was synthesized in order to functionalize PEG hydrogel coating around MIONPs. The binding of RGDS peptide to PEG was characterized via FTIR analysis. In the FTIR spectrum, the carbonyl groups (C=O) in NHS ester exhibits two peaks at 1781cm^{-1} and 1820 cm^{-1} [51]. After the conjugation reaction, the disappearance of these carbonyl bands points to that the NHS ester reacted with the amine groups in the RGDS structure and new amide bonds were formed as seen at figure 4.9-B. The peak corresponding to the carbonyl group in acryl-PEG-NHS was seen around 1740 cm^{-1}. After the conjugation reaction, amide I peak appeared at 1670cm^{-1} different from acryl-PEG-NHS [59]. This new peak is a clear evidence for the presence of RGDS in acryl-PEG-RGDS conjugate.

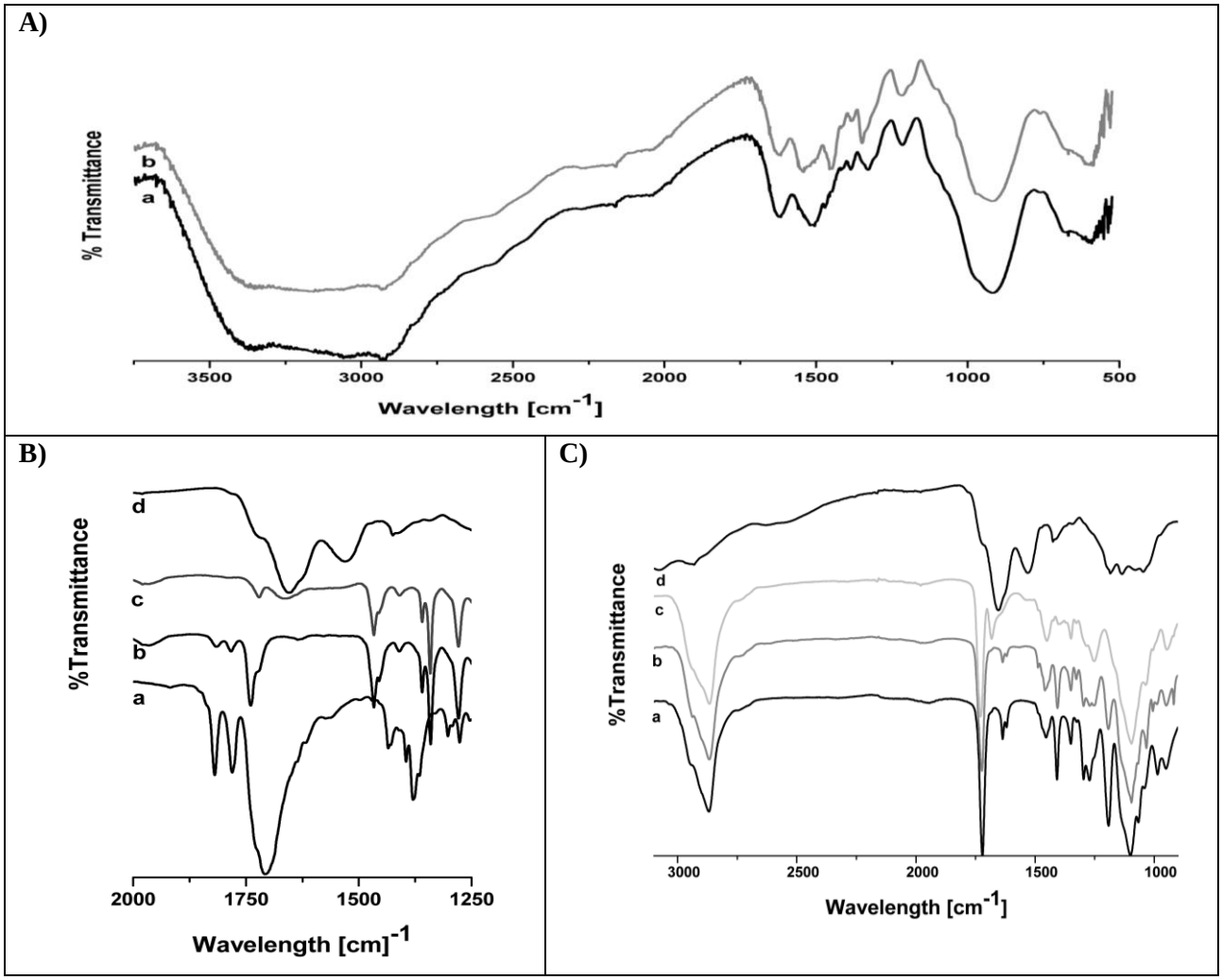

Figure 4.9 – FT-IR spectra A: a) APTMS-coated MIONP b) EY-bound MIONP; **B) a)** Acrylic acid NHS b) Acryl-PEG-NHS c) PEG-RGDS d) RGDS **C)** a) PEGDA b) PEG hydrogel encapsulated MIONPs c) RGDS functionalized PEG hydrogel encapsulated MIONPs d) RGDS

Table 4.1 – FT-IR spectra peaks of APTMS-coated or EY-bound MIONPs

FT-IR Peaks at the Spectra of APTMS Coated MIONPs [cm^{-1}]	Property	Ref.	FT-IR Peaks at the Spectra of APTMS Coated MIONPs [cm^{-1}]	Property	Ref.
571	**Magnetite Fe_2O_3**	[54]	572	**Magnetite Fe_2O_3**	[54]
590	**Magnetite Fe_2O_3**	[54]	591	**Magnetite Fe_2O_3**	[54]
919	**-CH out-of-plane bending**	[54]	918	**-CH out-of-plane bending**	[54]
1215	**Aliphatic C–N stretching**	[58]	1217	**Aliphatic C–N stretching**	[58]
1328	**Aliphatic C-O Stretching**	[58]	1348	**Aliphatic C-O Stretching**	[58]
1388	**Si-CH_2 (Scissoring)**	[57]	1383	**Si-CH_2(Scissoring)**	[57]
-			1456	**Aromatic C-C Stretching**	[58]
1505	**C-H Bending**	[58]	-		
-			1541	**Aromatic C=C Stretching**	[58]
1617	**NH_2 scissoring &N-H bending**	[58]	1617	**NH_2 scissoring &N-H bending**	[58]
2931	**CH_2 Stretching**	[54]	2931	**CH_2 Stretching**	[54]
3058	**NH_2 stretching**	[58]	-		
-			3156	**Secondary amide N-H stretching**	[58]
3352	**NH_2 stretching**	[58]	-		

FT-IR spectra of PEG hydrogel coated and RGDS functionalized PEG hydrogel coated MIONPs were shown at figure 4.9-C. After PEG hydrogel coating, new bands appeared at 1100 and 1352 cm^{-1} which were consistent with C-O-C stretching and C-O-C antisymmetric stretching, respectively. The peak at 950, 1724 and 2850 cm^{-1} were assigned to C-H out of plane bending, C=0 stretching and CH_2 stretching, respectively. In the FTIR spectra of PEG hydrogel coated samples, C=C stretching band at 1640 cm^{-1} mostly disappeared which contributed to the consumption of the double bonds during photocross-linking reaction. After addition of acryl-PEG-RGDS conjugate, amide I peak appeared at 1670cm^{-1} different from the case where no acryl-PEG-RGDS conjugate is present in the system.

Table 4.2 – FT-IR spectra peaks of PEGDA or PEG hydrogel

FT-IR Peaks at the Spectra of PEGDA	Property	Ref.	FT-IR Peaks at the Spectra of RGDS Functionalized PEG HG EMIONPs	Property	Ref.
950	C-H out of plane bending	[54]	950	C-H out of plane bending	[54]
1100	C-O-C Stretching	[54]	1100	C-O-C Stretching	[54]
1352	C-O-C antisymmetric stretching	[54]	1352	C-O-C antisymmetric stretching	[54]
1640	**C=C Stretching**	[X]	1640 (Mostly Disappeared)	**C=C Stretching**	[X]
1670	**-**		1670	Amide I Peak From RGDS	[60]
1724	C=0 Stretching	[58]	1724	C=0 Stretching	[58]
2850	CH_2- Stretching	[54]	2850	CH_2- Stretching	[54]

4.3.1.3. Determination of Hydrodynamic Size by DLS

In order to determine hydrodynamic diameter of different MIONPs, DLS has been used. The change in hydrodynamic size after EY binding and hydrogel coating on MIONP surface has been characterized. In addition the effect of pH on hydrodynamic size of the EY bound MIONP was investigated. The figure 4.10.-A demonstrates that pH variation from 6 to 8 did not alter hydrodynamic size distribution of EY bound MIONP, which shows that the concentration of H^+ ions in the system does not affect EY on MIONP surface and that EY has been covalently bound on MIONP surface. Size distribution of each MIONP has been shown in figure 4.10-B. Diameter of only APTMS coated NPs was 6.4 nm. After binding EY on NPs, diameter reached to 12.6 nm. When NPs were added into prepolymer solution (PPS), hydrodynamic size of NPs was 13.6 nm. The diameter of NPs became 23.3 nm after 20 sec laser exposure. Diameter increased to 58 nm and 122 nm, when laser exposure time was increased to 30 sec and 60 sec, respectively. When acryl-PEG-RGDS conjugate was added to the reaction, diameter of each sample was not changed significantly. The difference in hydrodynamic size before and after each modification were compared in figure 4.11-A.

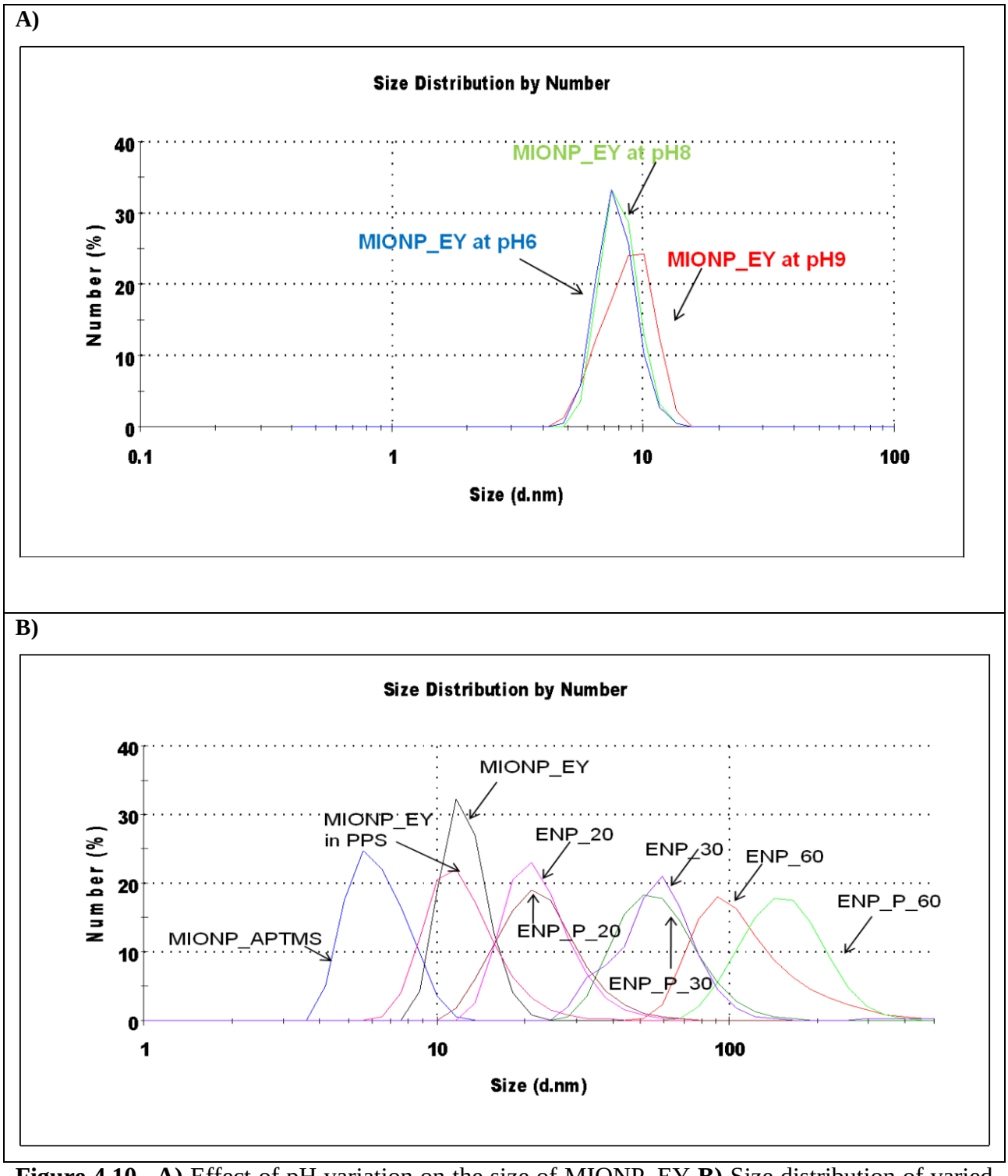

Figure 4.10– **A)** Effect of pH variation on the size of MIONP_EY **B)** Size distribution of varied MIONPs obtained via DLS (PPS: prepolymer solution, ENP: Encapsulated Nanoparticles, P: PEG-Peptide conjugate, Numbers correspond illumination time)

4.3.1.4. Colloidal Stability Characterization by Zeta Potential Measurement

Zeta potential measurement results show changes in surface charge of MIONPs during coating steps of NPs (figure 4.11-B). After negatively charged EY was bound on the MIONPs, charge of NPs changed from positive charge (+22.3 mV) to neutral (+2.3 mV). After encapsulation with PEG hydrogel, coated NPs became negatively charged (about -30 mV) which is the similar value obtained to PEGDA. Addition of PEG-RGDS conjugate did not affect surface charge significantly. The zeta potential values measured indicate that encapsulated NPs would have sufficient solution stability [61].

4.3.1.5. Morphology Analysis by AFM

After coating of MIONPs within PEG hydrogel, AFM has been used to support the presence of hydrogel on nanoparticle surface. MIONPs have been physically adsorbed on silicon surfaces and AFM imaging has been used, as could be observed in figure 4.12-A and B. APTMS coated MIONPs were stacked as multilayer according to figure 4.12-A. Phase picture of particles showed phase shift which can be attributed hard iron oxide particles on the silicon surface. Height picture of PEG hydrogel coated MIONPs demonstrated that most of particles were encapsulated individually, while several nanoparticles were encapsulated in cluster. When height picture and phase picture were compared, a core-shell-like structure of ENPs could be seen. The particles had inner magnetite core and outer polymeric shell of PEG. This provides additional evidence for the presence of PEG hydrogel on the surface of MIONPs.

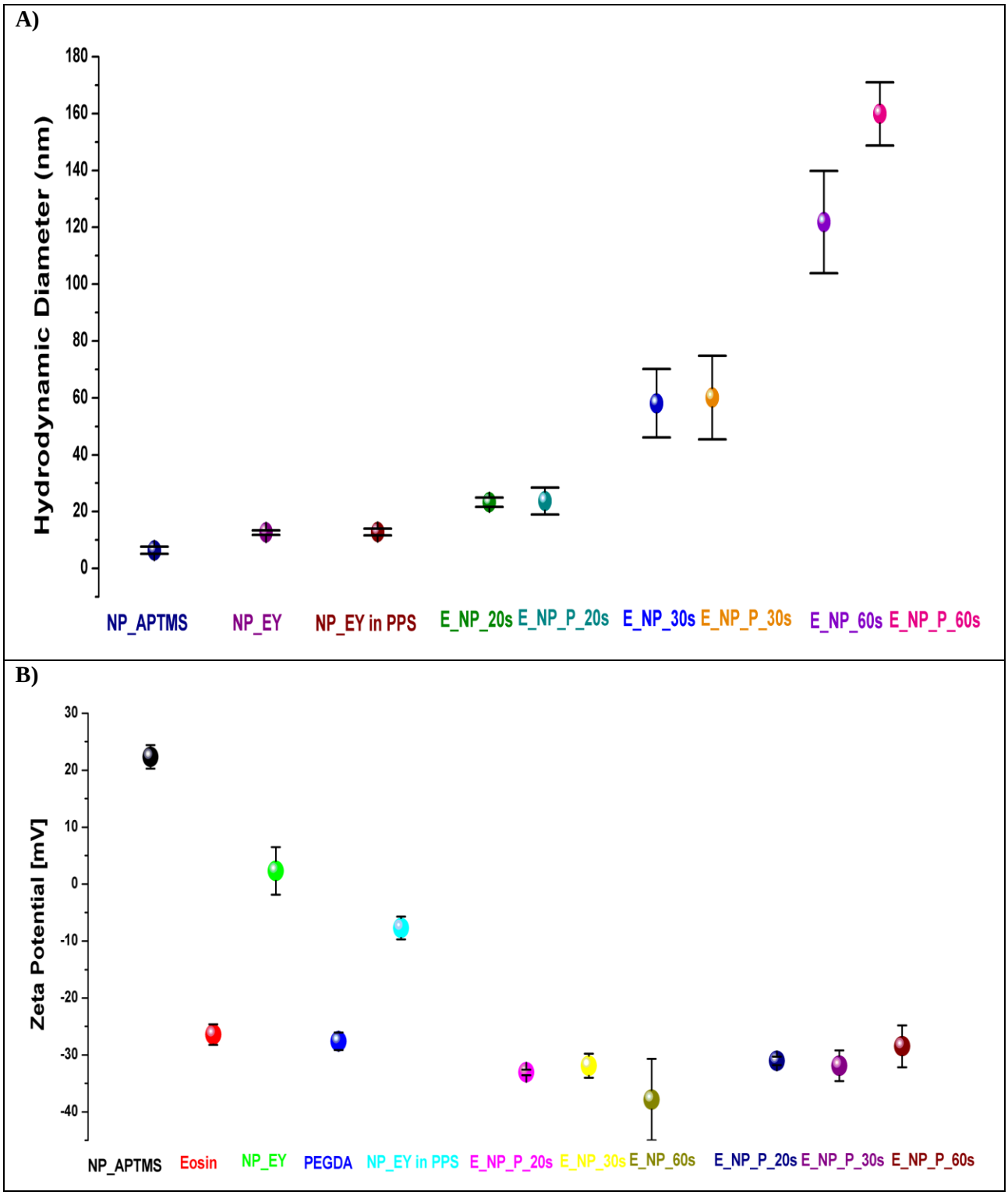

Figure 4.11 – A) Change of hydrodynamic diameter before and after PEG Hydrogel coating; B) ZETA potential measurement before and after PEG Hydrogel coating (PPS: prepolymer solution, ENP: Encapsulated Nanoparticles, P: PEG-Peptide conjugate, Numbers correspond illumination time)

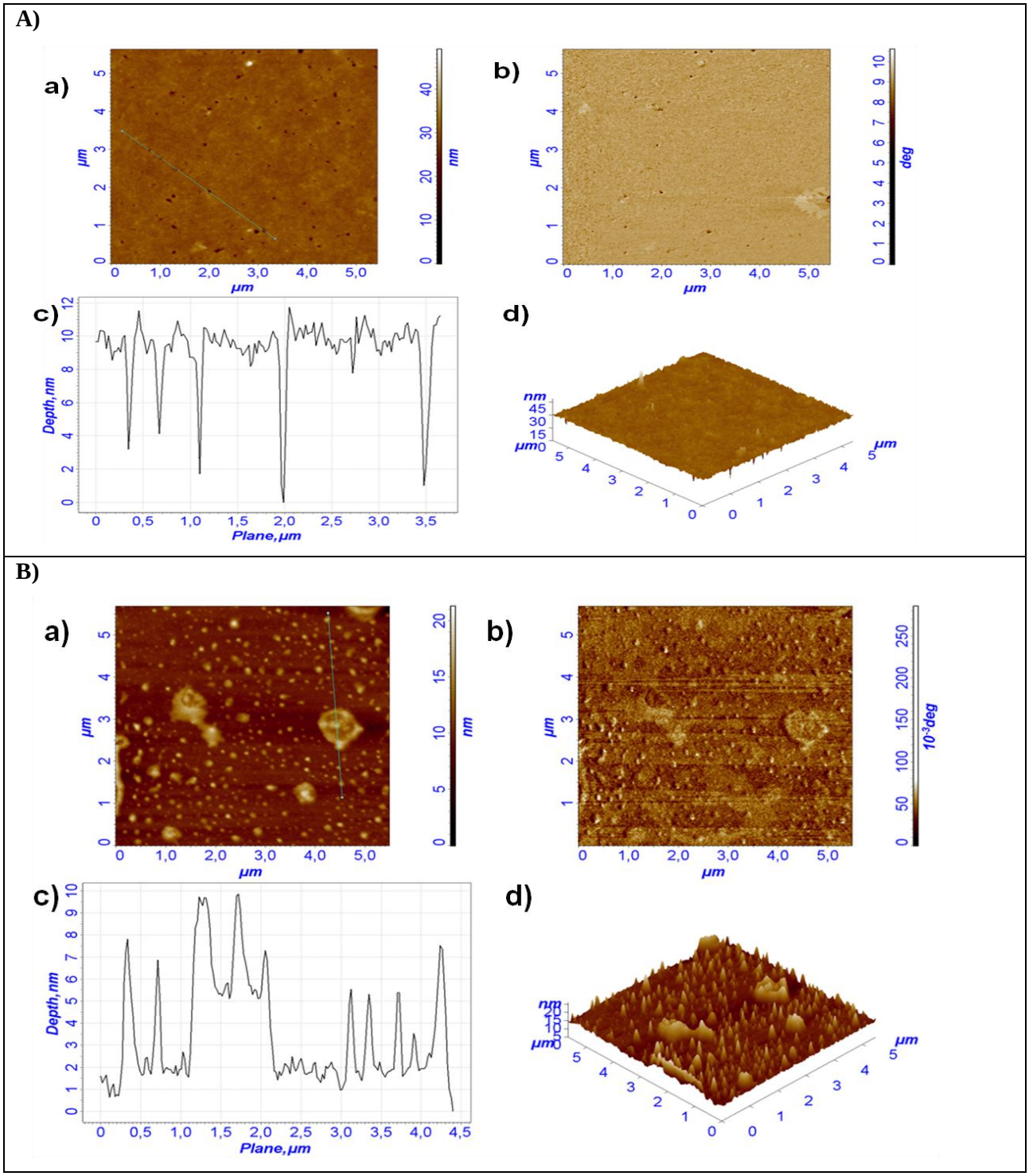

Figure 4.12 – A) AFM picture of APTMS coated MIONP: a) Height Picture, b) Phase Picture, c) Cross Section Analysis, d) Three Dimensional Representation. **B)** AFM Picture of 20 sec reacted Biofunctional PEG Hydrogel Coated MIONPs: a) Height Picture, b) Phase Picture, c) Cross Section Analysis, d)Three Dimensional Representation.

4.3.1.6. Cytotoxicity Analysis of MIONPs

In order to determine the toxicity of APTMS coated MIONPs, EY-bound MIONPs, PEG hydrogel coated MIONPs and biofunctional PEG hydrogel coated MIONPs, the viability of HeLa cells incubated with all types of MIONPs at 0.01, 0.05 and 0.10 mg/mL concentrations were examined using Cell-Titer-GLO Luminescent Viability Assay after 24 and 48 h treatment (figure 4.13). When we compare them with control sample that not contains any NPs, they did not show toxic effect at low concentration (0.01mg/mL). At higher concentration samples (0.05 and 0.1 mg/mL), EY bound and 20 sec reacted PEG hydrogel coated MIONP samples had toxic effect on both 24 h and 48 h cultured HeLa cells. If all free acrylate groups of PEGDA were saturated during photopolymerization, PEG Hydrogel coating did not affect cell viability. As a result, cellular metabolic activity in cells that were treated 30 sec and 60 sec reacted PEG hydrogel coated MIONPs did not change much in comparison with control cells because no significant diminish in the viability of the treated HeLa cells existed at the examined nanoparticle concentration.

4.3.1.7. Cellular Uptake of MIONPs

In order to compare cellular uptakes of varied MIONPs, Prussian blue staining and ICP methods were used. As is observed in figure 4.14, RGDS functionalized PEG hydrogel coated MIONPs demonstrated much stronger blue granule appearance, which is an direct indication of higher intracellular Fe concentration compared to the Fe concentration observed with both uncoated and only PEG hydrogel coated MIONPs.

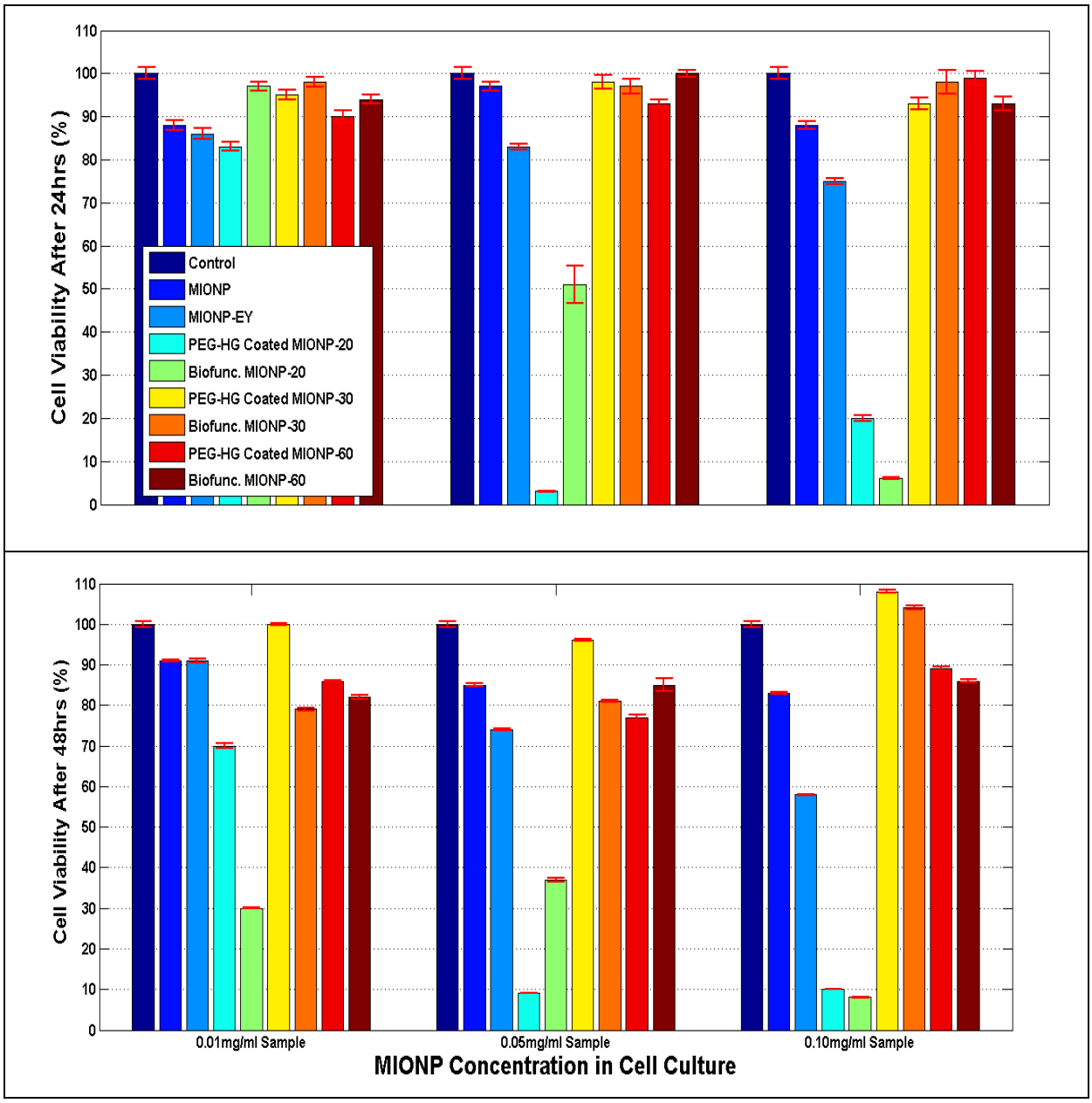

Figure 4.13 – Cytotoxicity profiles of varied MIONPs after 24 h and 48 h incubated with HeLa cells (Numbers correspond illumination time).

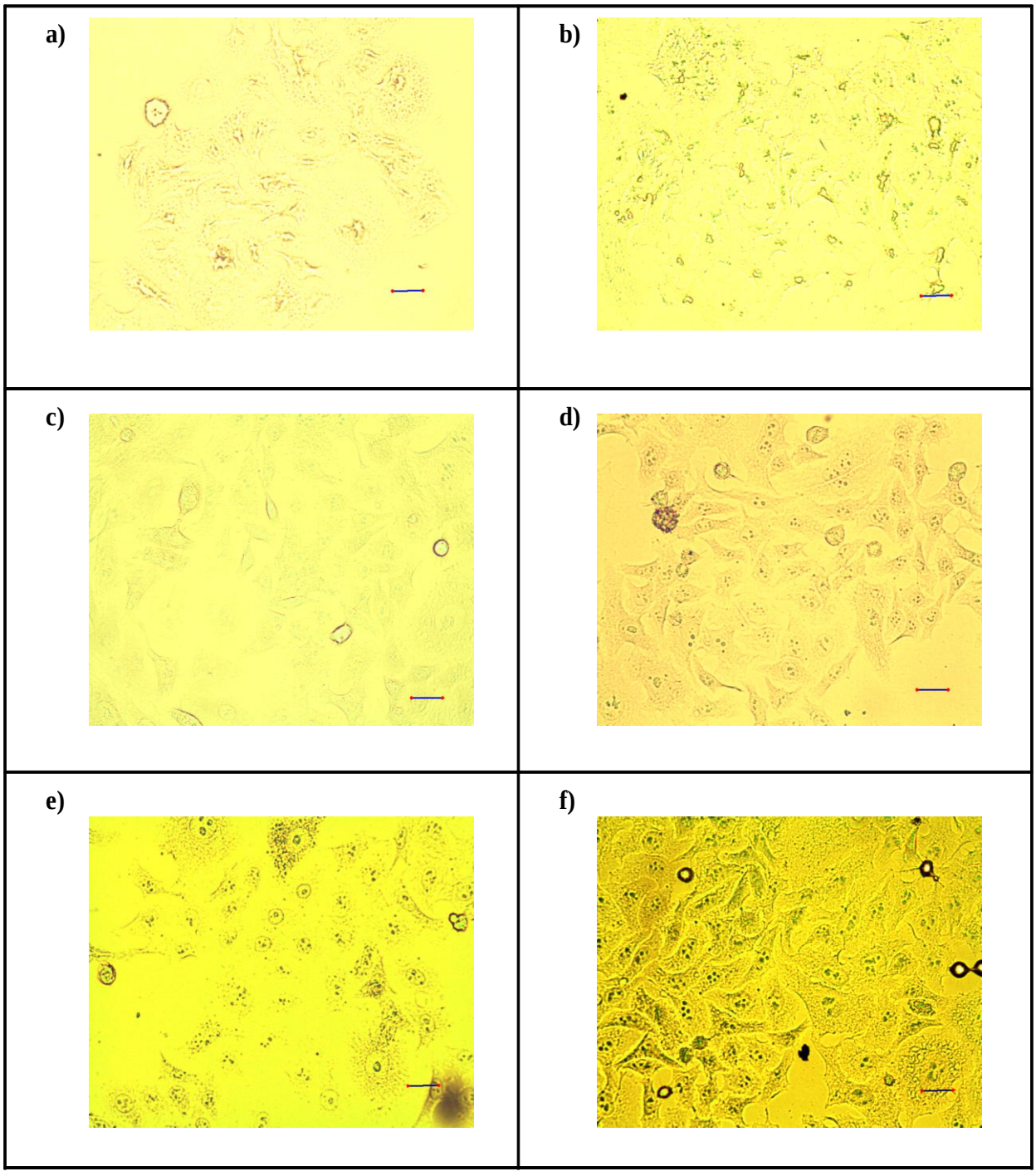

Figure 4.14 – Prussian blue stained HeLa cells: a) Control, b) MIONP_APTMS, c) PEG Hydrogel Coated-30, d) Biofunctional PEG Hydrogel Coated-30, e) PEG Hydrogel Coated-60, f) Biofunctional PEG Hydrogel Coated-60 (Scale Bar length: 25µm) (PPS: prepolymer solution, ENP: Encapsulated Nanoparticles, P: PEG-Peptide conjugate, Numbers correspond illumination time)

In addition, ICP result show higher numbers of RGDS functionalized PEG hydrogel coated MIONPs has been internalized into HeLa cells compared to the other conditions studied (60 sec illuminated and without PEG-RGDS conjugate PEG hydrogel coated MIONPs, 30 sec illuminated and with or without PEG-RGDS conjugate PEG hydrogel coated MIONPs, APTMS coated MIONPs) (figure 4.15). This suggests that, RGDS functionalization of PEG hydrogel may enhance cell targeting specifically.

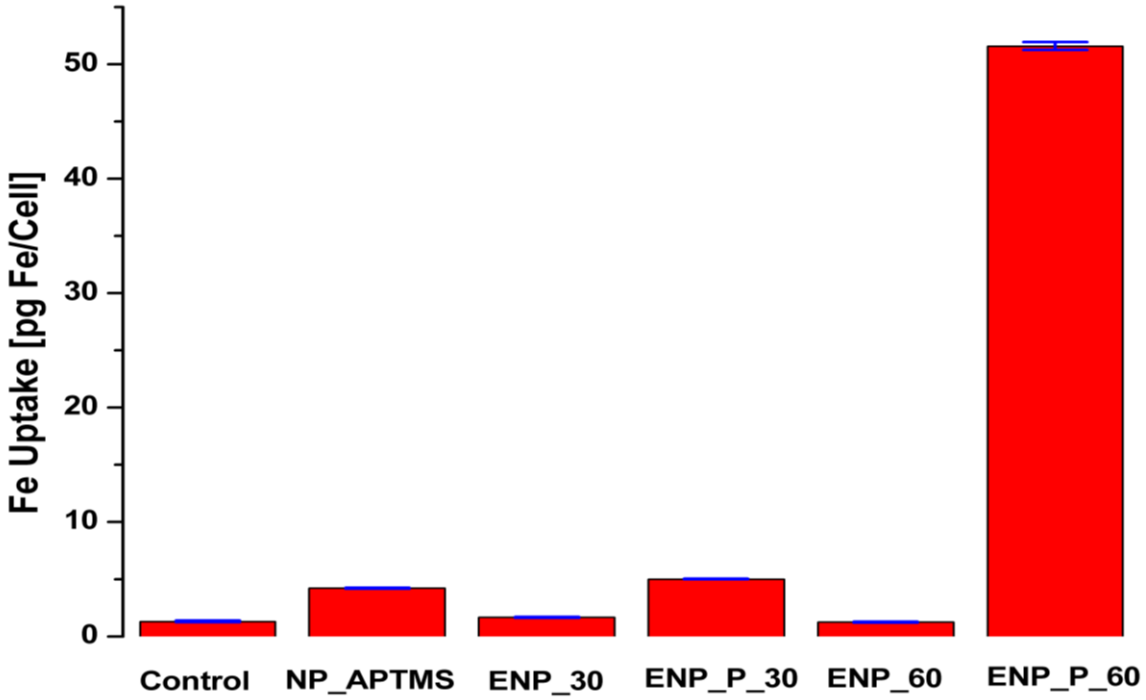

Figure 4.15 – Cellular uptake of varied MIONPs after 24 h obtained via ICP-OES (ENP: Encapsulated Nanoparticles, P: PEG-Peptide conjugate, Numbers correspond illumination time).

4.3.2. Discussion

Various strategies for coating MIONPs in order to prevent agglomeration and increase blood circulation time have been developed using natural and synthetic polymers such as alginate [55], dextran [62], liposome [63], PVP [39] and PEG[54, 56] . Polymeric coatings supply a steric barricade to prevent NPs agglomeration and avoid opsonization [12]. Some of the limitations involved in these approaches are lack of stabilization in body fluid, reaching targeted cell types, and enough of magnetic property. So, patients are exposed to high concentration of diagnosis or therapeutic agents. In order to address those limitations, encapsulation of MIONPs within biofunctional PEG hydrogel has been investigated in this study. Herein, *in vitro* results showed that this technique, based on surface initiated photopolymerization of PEGDA, does not compromise viability of HeLa cells. Further, biofunctionalization of PEG hydrogel coating of MIONPs increased the efficiency of cellular uptake of MIONPs considerably compared to the other conditions studied.

EY, which acts as a photoinitiator is bound covalently on APTMS-coated MIONPs with 57 % efficiency using WRK chemistry. Approximately 5 % of the total amine group of the MIONPs was modified via EY. EY concentration level which was bound on MIONPs was kept low because the modification of all amine group around MIONPs caused agglomeration of MIONPs (data not shown). It can be observed from figure 4.8-A and 4.9-A that carboxyl group in EY is bound to amine group of APTMS-coated MIONPs successfully when UV-Vis spectra and FT-IR spectra of both APTMS-coated and EY-bound MIONPs are compared.

Recent studies demonstrated that PEG coating minimizes intracellular uptake of NPs by macrophages [64] and increases circulation time in blood [65]. In this work, NPs were coated within hydrogel form of the PEG chains in order to enhance stability and water holding capacity of the coating. Furthermore, the usage of PEG hydrogel system allows a flexible skeleton for nanoparticle biofunctionalization because PEG-peptide or PEG-therapeutic agent can be incorporated into PEG hydrogel easily during photopolymerization in our technique. Cell membrane surface binding peptides are functional tools for targeting vascular endothelium in solid tumors to deliver therapeutic and imaging agents specifically [43]. Thus, covalent conjugation of cell attachment peptides into PEG hydrogel is a promising method to solve obstacles such as transportation and internalization of MIONPs to targeted specific cell types. In

this study, PEG hydrogel was functionalized via PEG-RGDS conjugate in order to enhance accumulation and internalization of MIONPs to cancer cells. The conjugation reaction between peptide and PEG was carried out successfully. It was verified by FT-IR spectroscopy. It can be identified from figure 4.9-B that apparent peaks of C=O stretching in NHS disappeared after attachment of the peptide to PEG. Also, amide I peak located at 1670cm^{-1} which corresponded peptide backbone [60] was noticeable at the spectrum related to PEG-RGDS.

PEG-RGDS conjugate and EY-bound MIONPs were added into the prepolymer solution and reacted via photopolymerization at mild conditions at different time intervals to adjust hydrogel thickness around MIONPs. According to figure 4.8-B, EY peak at 517 nm disappeared after the photopolymerization reaction. This result corresponded to bleaching of EY during light exposure. FT-IR spectra at figure 4.9-C illustrate that encapsulation of MIONPs within PEG hydrogel occurred profitably. The appearing the peaks regarding C-O-C, CH_2 and C-H give strong evidence that the MIONPs surface was covered with PEG hydrogel. According to FT-IR spectrum of the RGDS bound PEG hydrogel coated MIONPs, PEG-RGDS conjugate reacted successfully during photopolymerization reaction in order to produce biofunctional PEG hydrogel. In addition, high MW PEG was used as a spacer in conjugate structure to ease interaction between RGDS and integrins on the cell membrane.

Pharmacokinetics and cellular uptake of NPs are primarily based on physicochemical features of them such as hydrodynamic size, surface charge and morphology [42]. The hydrodynamic size of the particles before and after coating was characterized via DLS study which is based on analyzing the diffusion behavior of the NPs in solution [66]. According to the figure 4.10.-A, pH variation from 6 to 9 did not affect stabilization of EY-bound MIONP. Inspection of figure 4.10-B indicates that increasing illumination time could enlarge the thickness of the PEG hydrogel around MIONPs protecting narrow size distribution of APTMS coated MIONPs. Biofunctionalization of PEG hydrogel around MIONPs via adding PEG-RGDS in the polymerization reaction does not result in any difficulty in terms of size enlargement and distribution thunderingly. The electrostatic interactions of the NPs are able to be managed via adjustment of their surface charge that is analyzed via zeta potential measurement [67]. In this work, surface charge of MIONPs before and after coating was characterized via zeta potential measurement study. The altering surface charge of MIONPs throughout the coating modifications

was seen at figure 4.11-B in terms of zeta potential. These results demonstrate that PEG hydrogel coated MIONPs in aqueous solution can extend their durability satisfactorily without aggregation. It can be concluded from the zeta potential results that PEG hydrogel coating prevents aggregation in blood while circulating. The size and surface topography of APTMS-coated MIONPs and biofunctional PEG hydrogel coated MIONPs were characterized via AFM. It is evident from AFM results (figure 4.12-A and B) that MIONPs were coated within hydrogel layers effectively. However; some NPs were encapsulated in clusters instead of being individual because encapsulation of NPs in groups is not completely avoidable due to the close proximity of NPs within prepolymer solution. It is virtually certain that each encapsulated MIONPs had both inner iron oxide core and outer cross-linked PEG network. Size and surface modification of NPs could result in dissimilar response of cells to NPs in terms of non-specific or targeting cellular uptake [68]. Our method allows controllable size adjustment by changing illumination time and entrapment varied biomolecules into PEG hydrogel coating around MIONPs. Therefore, size or surface functionalization can be adapted to the targeting cell type.

Toxicity is a serious aspect which should be taken account while assessing performance of NPs for biomedical applications [69]. The initial step to analyze how NPs can react in human body requires cell-culture investigation [69]. Most of the cells die from cytotoxic agents after the initial 48 h treatment [69]. In our study, cell viability of the varied NPs exposed HeLa cells was evaluated via Cell-Titer-GLO Luminescent Viability Assay after 24 and 48 h treatment at different concentrations. Figure 4.13 shows that 30 sec and 60 sec reacted PEG hydrogel with and without RGDS encapsulated MIONPs had no significant effect on the cell viability compared with the control at all tested concentrations after both 24 h and 48 h treatment.

The capability to accumulate effectual concentrations of the agents to tumor area is a significant step of cancer diagnosis and treatment [70]. Ligand-receptor technique provides medical intervention to influence only cancer cells but not the healthy cells depending on molecular identification system [70]. This approach has great potential to enhance the efficiency of therapeutic and contrast agents by maximizing the amount of the agents around the targeted site, and to diminish cytotoxicity or imaging background signal by decreasing systemic subjection. Also, this method can identify the tumor at an earlier phase than current systems and eliminate an invasive biopsy requirement [70]. In this study, to demonstrate the ability of

biofunctional PEG hydrogel around MIONPs, intracellular uptake of various NPs was investigated applying both Prussian blue staining and ICP-OES measurement. The uptake of the NPs into HeLa cells was examined after 24 h treatment. It is illustrated from figure 4.14 that RGDS functionalized MIONPs internalize into the cancer cells much more than non-targeting MIONPs due to appearance of the considerably higher amount of blue granules after Prussian blue staining. Hence, microscopy observations were quantitatively supported analyzing intracellular iron content after the treatment via ICP-OES measurement. Figure 4.15 demonstrates noticeably that 60 sec-reacted and RGDS functionalized PEG hydrogel coated MINOPs internalized 10 times higher than APTMS-coated and only PEG hydrogel coated MIONPs. Based on cellular uptake results, it can be concluded that non-targeting PEG hydrogel encapsulation minimizes cellular interaction and unspecific cellular uptake, while targeting PEG hydrogel encapsulation provides high accumulation of MIONPs into cancer cells. Therefore, in addition to diagnostic agent property of MIONPs, the entrapment of chemotherapeutic agents into our MIONPs formulations can eliminate side effects of the agents whereas improving the accumulation of the agents into cancer tissues. Furthermore, RGDS functionalized PEG hydrogel coated MIONPs are promising for usage in hyperthermia therapy which is a method to raise temperature locally at tumor area when MIONPs are exposed with external magnetic field [35, 46]. This technique also requires optimal particle size and targeting tumor to kill cancer cells efficiently by heating.

NPs must be fast, specific and effective in terms of reaching and uptake into target cells [71]. Their performance *in vivo* is restricted by several factors such as aggregation, short half-life in blood circulation, inefficient cellular uptake and non-specific targeting [71]. MIONPs should be coated with biocompatible materials in a size-controllable form to overcome difficulties against transportation and internalization of MIONPs to targeted specific cell types. It is believed that biofunctional PEG hydrogel coating technology may be capable of provide requirements that are related to desired MIONPs performance *in vivo*. This approach may not only allow target specific tissues in the body, but also may permit the decrease of the quantity of diagnostic or therapeutic agents needed to accomplish a particular concentration in the surroundings of the targeted tissues. Hence, it can diminish the exposure of the agents to non-targeted tissues whereas attenuating severe side effects.

Chapter 5

CONCLUSION

Two types of biofunctional PEG hydrogel systems were investigated: one is encapsulation of islets as within this biofunctional membrane to provide immunoisolation, and the other is the coating of MIONPs within this membrane to enhance tumor detection.

In the first part of the study, islets were individually encapsulated within insulinotropic ligand functionalized PEG hydrogel via surface initiated photopolymerization technique. Mild photopolymerization conditions and GLP-1 functionalized PEG hydrogel coating provide elimination of cytotoxicity and loss of functionality. Encapsulation of pancreatic islets within biofunctional PEG hydrogel is a promising technique to bring islet encapsulation technology to a clinical reality.

In the second part of this study, MIONPs were encapsulated within cell adhesion ligand functionalized nano-thin PEG hydrogels. In recent years, MIONPs have been improved with the purpose of diagnosis and treatment of diseases as well as *in vitro* applications such as magnetic separation of cells, proteins, DNA/RNA, and other biomolecules. MIONPs hold enormous potential of creating new preferences for early cancer detection and targeted therapies. In order to overcome limitations of MIONP technologies, we have improved a novel strategy that is useful for encapsulation and functionalization of MINOPs. It is a significant candidate to develop desired MIONPs that demonstrate enhanced magnetic properties and biocompatible, biofunctional as well as multifunctional features. Encapsulated MIONPs within biofunctional PEG hydrogel could prevent agglomeration and increase blood circulation time which will be significant tool for diagnostic and therapeutic imaging technologies as well as targeted drug delivery area. In this process, after intravenous injection of biofunctional PEG hydrogel coated MIONPs, magnetic field gradient is applied to direct them to the tumor tissue. Next, cell adhesion ligand can provide internatization of NPs into cancer cells specifically. This method is not only

applicable for the iron oxide nanoparticles, but also it can be extended to encapsulate nanoparticles with different geometries such as nanotubes or nanorods.

Finally, encapsulation of islets or NPs within biofunctional PEG hydrogel using the strategies presented in this work may significantly advance current existing approaches in these fields. Future work includes the investigation of immunoisolation capability of GLP-1 functionalized PEG hydrogel coating *in vitro* and *in vivo.* At the encapsulation part of the study, exact diameter as well as magnetic property *in vitro* and *in vivo* of the ENPs will be determined.

BIBLIOGRAPHY

1. Baroli, B., *Hydrogels for tissue engineering and delivery of tissue-inducing substances.* J Pharm Sci, 2007. **96**(9): p. 2197-223.
2. Oh, J.K., et al., *The development of microgels/nanogels for drug delivery applications.* Progress in Polymer Science, 2008. **33**(4): p. 448-477.
3. Kizilel, S., V.H. Perez-Luna, and F. Teymour, *Photopolymerization of poly(ethylene glycol) diacrylate on eosin-functionalized surfaces.* Langmuir, 2004. **20**(20): p. 8652-8.
4. Burdick, J.A. and K.S. Anseth, *Photoencapsulation of osteoblasts in injectable RGD-modified PEG hydrogels for bone tissue engineering.* Biomaterials, 2002. **23**(22): p. 4315-23.
5. Cruise, G.M., et al., *In vitro and in vivo performance of porcine islets encapsulated in interfacially photopolymerized poly(ethylene glycol) diacrylate membranes.* Cell Transplant, 1999. **8**(3): p. 293-306.
6. Meenach, S.A., J.Z. Hilt, and K.W. Anderson, *Poly(ethylene glycol)-based magnetic hydrogel nanocomposites for hyperthermia cancer therapy.* Acta Biomater, 2010. **6**(3): p. 1039-46.
7. Hoffman, A.S., *Hydrogels for biomedical applications.* Adv Drug Deliv Rev, 2002. **54**(1): p. 3-12.
8. Lee, D.Y., et al., *A new strategy toward improving immunoprotection in cell therapy for diabetes mellitus: long-functioning PEGylated islets in vivo.* Tissue Eng, 2006. **12**(3): p. 615-23.
9. Kizilel, S., et al., *Encapsulation of pancreatic islets within nano-thin functional polyethylene glycol coatings for enhanced insulin secretion.* Tissue Eng Part A, 2010. **16**(7): p. 2217-28.
10. Hern, D.L. and J.A. Hubbell, *Incorporation of adhesion peptides into nonadhesive hydrogels useful for tissue resurfacing.* J Biomed Mater Res, 1998. **39**(2): p. 266-76.
11. Mahmoudi, M., A. Simchi, and M. Imani, *Recent Advances in Surface Engineering of Superparamagnetic Iron Oxide Nanoparticles for Biomedical Applications.* Journal of the Iranian Chemical Society, 2010. **7**: p. S1-S27.

12. Sun, C., J.S. Lee, and M. Zhang, *Magnetic nanoparticles in MR imaging and drug delivery.* Adv Drug Deliv Rev, 2008. **60**(11): p. 1252-65.
13. Nitin, N., et al., *Functionalization and peptide-based delivery of magnetic nanoparticles as an intracellular MRI contrast agent.* J Biol Inorg Chem, 2004. **9**(6): p. 706-12.
14. Brubaker, P.L. and D.J. Drucker, *Minireview: Glucagon-like peptides regulate cell proliferation and apoptosis in the pancreas, gut, and central nervous system.* Endocrinology, 2004. **145**(6): p. 2653-9.
15. Barbucci, R., *Hydrogels : biological properties and applications*. 2009, Milan ; New York: Springer. xi, 197 p.
16. Ratner, B.D. and S.J. Bryant, *Biomaterials: where we have been and where we are going.* Annu Rev Biomed Eng, 2004. **6**: p. 41-75.
17. Hamidi, M., A. Azadi, and P. Rafiei, *Hydrogel nanoparticles in drug delivery.* Advanced Drug Delivery Reviews, 2008. **60**(15): p. 1638-1649.
18. Zhu, J., *Bioactive modification of poly(ethylene glycol) hydrogels for tissue engineering.* Biomaterials, 2010. **31**(17): p. 4639-56.
19. Tomme, S.V., *Self-assembling microsphere-based dextran hydrogels for pharmaceutical applications* in *Department of Pharmaceutics*. 2007, Utrecht University: Utrecht. p. 188.
20. Datta, A., *Characterization of polyethylene glycol hydrogels for Biomedical applications*, in *Chemical Engineering* 2007, B.E. University of Pune. p. 107.
21. JIN HO LEE, H.B.L.A.J.D.A., *BLOOD COMPATIBILITY OF POLYETHYLENE OXIDE SURFACES.* Progress in Polymer Science, 1995. **20**: p. 1043-1079.
22. Heuts, J.P.A., *Theory of Radical Polymerization*, in *Handbook of Radical Polymerization*, K.M.a.T.P. Davis, Editor. 2002, Wiley-Interscience. p. 1-76.
23. Fisher, J.P., et al., *Photoinitiated polymerization of biomaterials.* Annual Review of Materials Research, 2001. **31**: p. 171-181.
24. Sokmen, N., F. Ayhan, and H. Ayhan, *POLY 488-Gelatin containing photopolymerized poly(ethylene glycol) diacrylate hydrogels for drug delivery.* Abstracts of Papers of the American Chemical Society, 2008. **236**.
25. Kizilel, S., M. Garfinkel, and E. Opara, *The bioartificial pancreas: progress and challenges.* Diabetes Technol Ther, 2005. **7**(6): p. 968-85.

26. Bluestone, J.A., K. Herold, and G. Eisenbarth, *Genetics, pathogenesis and clinical interventions in type 1 diabetes.* Nature, 2010. **464**(7293): p. 1293-300.
27. Adams, D.D., J.G. Knight, and A. Ebringer, *Autoimmune diseases: Solution of the environmental, immunological and genetic components with principles for immunotherapy and transplantation.* Autoimmun Rev, 2010. **9**(8): p. 525-30.
28. Beck, J., et al., *Islet encapsulation: strategies to enhance islet cell functions.* Tissue Eng, 2007. **13**(3): p. 589-99.
29. Mahato, R.I., et al., *Cationic lipid and polymer-based gene delivery to human pancreatic islets.* Mol Ther, 2003. **7**(1): p. 89-100.
30. Naftanel, M.A. and D.M. Harlan, *Pancreatic islet transplantation.* PLoS Med, 2004. **1**(3): p. e58; quiz e75.
31. Kang, H.C. and Y.H. Bae, *Transfection of rat pancreatic islet tissue by polymeric gene vectors.* Diabetes Technol Ther, 2009. **11**(7): p. 443-9.
32. Lanza, R.P., R.S. Langer, and J. Vacanti, *Principles of tissue engineering*. 3rd ed. 2007, Amsterdam ; Boston: Elsevier / Academic Press. xxvii, 1307 p.
33. Wyman, J.L., et al., *Immunoisolating pancreatic islets by encapsulation with selective withdrawal.* Small, 2007. **3**(4): p. 683-90.
34. Sanborn, T.J., P.B. Messersmith, and A.E. Barron, *In situ crosslinking of a biomimetic peptide-PEG hydrogel via thermally triggered activation of factor XIII.* Biomaterials, 2002. **23**(13): p. 2703-10.
35. Jung Kwon Oh, J.M.P., *Iron Oxide-based Superparamagnetic Polymeric Nanomaterials: Design, Preparation, and Biomedical Application.* Progress in Polymer Science, 2010.
36. Hu, F., et al., *Cellular response to magnetic nanoparticles "PEGylated" via surface-initiated atom transfer radical polymerization.* Biomacromolecules, 2006. **7**(3): p. 809-16.
37. Gupta, A.K. and M. Gupta, *Synthesis and surface engineering of iron oxide nanoparticles for biomedical applications.* Biomaterials, 2005. **26**(18): p. 3995-4021.
38. Cole, A.J., et al., *Polyethylene glycol modified, cross-linked starch-coated iron oxide nanoparticles for enhanced magnetic tumor targeting.* Biomaterials, 2011. **32**(8): p. 2183-93.

39. Lee, H.Y., et al., *Preparation and magnetic resonance imaging effect of polyvinylpyrrolidone-coated iron oxide nanoparticles.* J Biomed Mater Res B Appl Biomater, 2006. **79**(1): p. 142-50.

40. Tong, S., et al., *Coating Optimization of Superparamagnetic Iron Oxide Nanoparticles for High T(2) Relaxivity.* Nano Lett, 2010.

41. Acar, H.Y.C., et al., *Superparamagnetic nanoparticles stabilized by polymerized PEGylated coatings.* Journal of Magnetism and Magnetic Materials, 2005. **293**(1): p. 1-7.

42. Veiseh, O., J.W. Gunn, and M. Zhang, *Design and fabrication of magnetic nanoparticles for targeted drug delivery and imaging.* Adv Drug Deliv Rev, 2010. **62**(3): p. 284-304.

43. Kessler, T., et al., *Inhibition of tumor growth by RGD peptide-directed delivery of truncated tissue factor to the tumor vasculature.* Clin Cancer Res, 2005. **11**(17): p. 6317-24.

44. Puleo, D.A. and R. Bizios, *RGDS tetrapeptide binds to osteoblasts and inhibits fibronectin-mediated adhesion.* Bone, 1991. **12**(4): p. 271-6.

45. Zhang, C., et al., *Specific targeting of tumor angiogenesis by RGD-conjugated ultrasmall superparamagnetic iron oxide particles using a clinical 1.5-T magnetic resonance scanner.* Cancer Res, 2007. **67**(4): p. 1555-62.

46. Gupta, A.K., et al., *Recent advances on surface engineering of magnetic iron oxide nanoparticles and their biomedical applications.* Nanomedicine (Lond), 2007. **2**(1): p. 23-39.

47. Kizilel, S., V.H. Perez-Luna, and F. Teymour, *Mathematical model for surface-initiated photopolymerization of poly(ethylene glycol) diacrylate.* Macromolecular Theory and Simulations, 2006. **15**(9): p. 686-700.

48. Duvivier-Kali, V.F., et al., *Complete protection of islets against allorejection and autoimmunity by a simple barium-alginate membrane.* Diabetes, 2001. **50**(8): p. 1698-705.

49. Teramura, Y. and H. Iwata, Biomaterials 2009. **30**: p. 2270-2275.

50. Kizilel, S., *Mathematical Model for Microencapsulation of Pancreatic Islets within a Biofunctional PEG Hydrogel.* Macromol Theory Simul, 2010. **19**(8-9): p. 514-531.

51. Kim, H., et al., Polym Advan Technol, 2009. **20**: p. 298.

52. Toso, C., et al., *Intra-portal injection of 400-um microcapsules in a large-animal model.* Transplant International, 2003. **16**(6): p. 405-410.

53. Varo, G., et al., *Binding of calcium ions to bacteriorhodopsin.* Biophys J, 1999. **76**(6): p. 3219-26.

54. Gupta, A.K. and S. Wells, *Surface-modified superparamagnetic nanoparticles for drug delivery: preparation, characterization, and cytotoxicity studies.* IEEE Trans Nanobioscience, 2004. **3**(1): p. 66-73.

55. Ma, H.L., et al., *Preparation and characterization of superparamagnetic iron oxide nanoparticles stabilized by alginate.* Int J Pharm, 2007. **333**(1-2): p. 177-86.

56. Park, J.Y., et al., *Highly water-dispersible PEG surface modified ultra small superparamagnetic iron oxide nanoparticles useful for target-specific biomedical applications.* Nanotechnology, 2008. **19**(36): p. 365603.

57. Mikhaylova, M., et al., *BSA immobilization on amine-functionalized superparamagnetic iron oxide nanoparticles.* Chemistry of Materials, 2004. **16**(12): p. 2344-2354.

58. Stuart, B., *Infrared spectroscopy : fundamentals and applications*. Analytical techniques in the sciences. 2004, Chichester, West Sussex, England ; Hoboken, NJ: J. Wiley. xv, 224 p.

59. Porjazoska, A., et al., *Synthesis and characterization of poly(ethylene glycol)-poly(D,L-lactide-co-glycolide) poly(ethylene glycol) tri-block co-polymers modified with collagen: a model surface suitable for cell interaction.* J Biomat Sci Polym Ed, 2006. **17**(3): p. 323-340.

60. Berthomieu, C. and R. Hienerwadel, *Fourier transform infrared (FTIR) spectroscopy.* Photosynth Res, 2009. **101**(2-3): p. 157-70.

61. Gogo*t*si, I.U.G., *Nanomaterials handbook*. 2006, Boca Raton: CRC/Taylor & Francis. 780 p.

62. Moore, A., et al., *Tumoral distribution of long-circulating dextran-coated iron oxide nanoparticles in a rodent model.* Radiology, 2000. **214**(2): p. 568-74.

63. Liao, Z., et al., *Polymeric Liposomes-Coated Superparamagnetic Iron Oxide Nanoparticles as Contrast Agent for Targeted Magnetic Resonance Imaging of Cancer Cells.* Langmuir, 2011.

64. Zhang, Y., N. Kohler, and M. Zhang, *Surface modification of superparamagnetic magnetite nanoparticles and their intracellular uptake.* Biomaterials, 2002. **23**(7): p. 1553-61.

65. Gref, R., et al., *Biodegradable long-circulating polymeric nanospheres.* Science, 1994. **263**(5153): p. 1600-3.

66. Wang, Y.X., S.M. Hussain, and G.P. Krestin, *Superparamagnetic iron oxide contrast agents: physicochemical characteristics and applications in MR imaging.* Eur Radiol, 2001. **11**(11): p. 2319-31.

67. Ge, Y., et al., *Effect of surface charge and agglomerate degree of magnetic iron oxide nanoparticles on KB cellular uptake in vitro.* Colloids Surf B Biointerfaces, 2009. **73**(2): p. 294-301.

68. Wu, X., et al., *Toxic effects of iron oxide nanoparticles on human umbilical vein endothelial cells.* Int J Nanomedicine, 2010. **5**: p. 385-99.

69. Lewinski, N., V. Colvin, and R. Drezek, *Cytotoxicity of nanoparticles.* Small, 2008. **4**(1): p. 26-49.

70. Koo, Y.E., et al., *Brain cancer diagnosis and therapy with nanoplatforms.* Adv Drug Deliv Rev, 2006. **58**(14): p. 1556-77.

71. Margarethe Hofmann-Amtenbrink, B.v.R., and Heinrich Hofmann, *Superparamagnetic nanoparticles for biomedical applications*, in *Nanostructured Materials for Biomedical Applications*, M.C. Tan, Editor. 2009, Transworld Research Network: Kerala.

VITA

Caner Nazlı was born in Istanbul, Turkey in 1986. He was graduated from Ankara Ataturk Anadolu Lisesi in 2004. Same year, he started Molecular Biology and Genetic Department at Istanbul Technical University, Istanbul. In 2009, he received his B.S. degree and joined Material Science and Engineering Program at Koç University. His current research interest is to encapsulate cells / nanoparticles within biofunctional PEG hydrogel for biomedical applications.